Hydrogen Bonded Phenols as Models for Redox-Active Tyrosines in Enzymes

Josefin Utas

Doctoral Dissertation May 2006

Dept. of Organic Chemistry
Arrhenius Laboratory
Stockholm University
Stockholm, Sweden

Abstract

This thesis deals with the impact of hydrogen bonding on the properties of phenols. The possibility for tyrosine to form hydrogen bonds to other amino acids has been found to be important for its function as an electron transfer mediator in a number of important redox enzymes. This study has focused on modeling the function of tyrosine in Photosystem II, a crucial enzyme in the photosynthetic pathway of green plants.

Hydrogen bonds between phenol and amines in both inter- and intramolecular systems have been studied with quantum chemical calculations and also in some solid-state structures involving phenol and imidazole.

Different phenols linked to amines have been synthesized and their possibilities of forming intra- and intermolecular hydrogen bonds have been studied as well as the thermodynamics and kinetics of the generation of phenoxyl radicals via oxidation reactions.

Since carboxylates may in principle act as hydrogen bond acceptors in a manner similar to imidazole, proton coupled electron transfer has also been studied for a few phenols intramolecularly hydrogen bonded to carboxylates with the aim to elucidate the mechanism for oxidation. Electron transfer in a new linked phenol—ruthenium(II)trisbipyridine complex was studied as well.

The knowledge is important for the ultimate goal of the project, which is to transform solar energy into a fuel by an artificial mimic of the natural photosynthetic apparatus.

ISBN: 91-7155-278-2
US-AB, Universitetsservice

List of Publications

The thesis is based on the following papers, referred to in the text by their Roman numerals I-V.

I. Solid-State Structures with Hydrogen Bonds between Phenol and Imidazole as Models for Tyrosine and Histidine in Proteins

Josefin E. Utas, Mikael Kritikos, Sergey V. Dvinskikh, Dick Sandström, and Björn Åkermark.

Submitted to *J.Phys. Chem.*

II. Water as a Hydrogen Bonding Bridge between a Phenol and Imidazole. A Simple Model for Water Binding in Enzymes.

Josefin E. Utas, Mikael Kritikos, Dick Sandström, Björn Åkermark.

Submitted to *Biochim. Biophys. Acta.*

III. Efficient Synthesis of 2-Substituted Imidazoles by Palladium-Catalyzed Cross-Coupling with Benzylzinc Reagent

Josefin E. Utas, Berit Olofsson, Björn Åkermark.

Sumitted to *Synlett*.

IV. The Effect of Imidazole on Phenol Oxidation – Models for Tyr_Z and His190 in Photosystem II

Josefin E. Utas, Tania Irebo, Reiner Lomoth, Martin Sjödin, Licheng Sun, Cecilia Tommos, Margareta Blomberg, Leif Hammarström, Björn Åkermark**.**

Manuscript.

V. Kinetic Effects of Hydrogen-bonds on Proton-Coupled Electron Transfer from Phenols

Martin Sjödin, Tania Irebo, Josefin E. Utas, Johan Lind, Gabor Merényi, Björn Åkermark, Leif Hammarström.

J. Am. Chem Soc. Revised manuscript submitted.

Abbreviations and Symbols

A	acceptor
Asp	aspartic acid
ATP	adenosine triphosphate
B3LYP	a hybrid density functional method
BSSE	basis set superposition error
bpy	[2,2']-bipyridine
CEP	concerted electron and proton transfer
CP	cross polarization
CV	cyclic voltammetry
D	donor
DFT	density functional theory
DPV	differential pulse voltammetry
E^0	standard potential
$E^{0'}$	formal potential
ET	electron transfer
ETPT	electron transfer-proton transfer
Fc	ferrocene
Gln	glutamine
Glu	glutamic acid
His	histidine
I_{HB}	hydrogen bond interaction energy
Im	imidazole
IP	ionization potential
k	rate constant for electron transfer
MAS	magic angle spinning
MLCT	metal to ligand charge transfer
MV^{2+}	methyl viologen
NADPH	nicotinamide adenine dinucleotide phosphate
NHE	normal hydrogen electrode
PCET	proton-coupled electron transfer
Pheo	pheophytin
PhO^-	deprotonated phenol
$PhO^{\bullet}$	neutral phenoxyl radical
$PhOH^{\bullet+}$	phenoxyl radical cation
PhOH	phenol
PSII	photosystem II
PTET	proton transfer-electron transfer
Q	quinone
RAHB	resonance assisted hydrogen bond
SEM	2-(trimethylsilyl)ethoxymethyl group
Tyr	tyrosine

Table of contents

1 Introduction

Nature's complexity is enormous. The vast variety of different organisms and the strategies they have developed to survive, even in the most hostile environments, are invaluable sources of information for us humans. The study and understanding of nature's principles can provide mankind with new ideas and inspiration for how to improve our lives. However, to be able to use this information actively to invent new technology, we have to understand exactly why and how nature is doing the things it does. This is not an easy task.

One of the greatest challenges in our time is to find new environmentally friendly energy sources to replace nuclear power and fossil fuels. The biggest source of energy on earth has long been photosynthesis, that is, the capturing and storage of solar energy. Mimicking this process in a simple man-made system is an appealing way to solve the energy-problem. Energy from a catalytic cycle in which water is split by sunlight without any production of waste, could be the result.

The heart of photosynthesis, photosystem II, is a light-harvesting enzyme that performs the central reaction in the process: the splitting of water to form oxygen. This is a redox reaction and the whole process therefore involves multistep electron transfer between different redox co-factors.

This work is devoted to studying the properties and the function of model systems for the so-called tyrosine-z, a phenolic redox co-factor that plays a crucial role in photosystem II, with the ultimate goal of learning how to incorporate tyrosine-models in artificial systems. Since the details of all steps in the complete process are not entirely clarified yet, the information gained in model systems also gives input to the studies of the parent system, photosystem II.

2 Background

2.1 Natural photosynthesis

Photosynthesis is the process in which sun light is used by green plants, algae and cyanobacteria to form carbohydrates and oxygen from carbon dioxide and water (eq. 2.1).

$$6H_2O + 6CO_2 + \text{sunlight} \rightarrow C_6H_{12}O_6 + 6O_2 \qquad (2.1)$$

The process takes place in the chloroplasts of the cells, employing a collection of protein complexes situated in the thylakoid membrane that is separating the inner part, the lumen, from the outer part, the stroma. In green plants, the light processes are performed by two large protein complexes called photosystem I and photosystem II (PSI and PSII), which harvest sunlight at different wave-

lengths. The details of all the steps involved are unknown but the main features are fairly well understood.

In PSII light is absorbed by an antenna system consisting of chlorophyll molecules (Figure 2.1). The energy is funneled to a special pair of chlorophyll molecules called P680 in green plants. The excitation of P680 triggers an electron transfer to a nearby electron acceptor, thus creating the first charge separated state.[1] A series of electron transfer steps follows and the energy is eventually transformed into NADPH and ATP that will be used by the organism for its energy supply. To facilitate the electron transfer, every step is slightly downhill in energy. The strategy of employing a multistep electron transfer cascade assures that the electron and the hole are separated by large distances and that the back-electron transfer, which would result in a loss of the absorbed energy, is avoided.

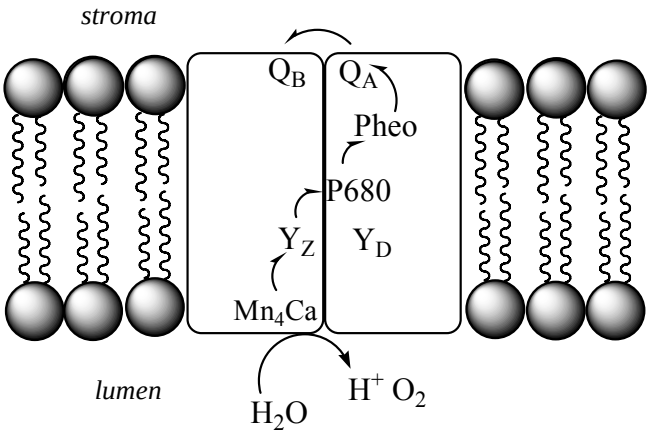

Figure 2.1 Schematic picture of the electron transport in photosystem II.

The photo-oxidized form of P680, $P680^+$, is reduced by electrons originating from water, the oxidation of which takes place in a metal-cluster consisting of four manganese ions and one calcium ion. At the cluster, often referred to as the OEC (oxygen evolving complex), oxygen gas is produced. The metal-ions are mainly ligated by amino acids with carboxylic acid side chains. The electron transfer between the manganese cluster and P680 proceeds via a single radical co-factor, the tyrosine residue D1-Y161, called Tyr_z or Y_z. The separation of Tyr_Z and Ca^{2+} is 4.9 Å.[2] Y_D is another redo-active tyrosine residue, not directly involved in water oxidation (see chapter 2.5.1).

The reaction catalyzed by the Mn-cluster is depicted in eq. 2.2. To release one molecule of oxygen, two molecules of water have to be oxidized.

$$2H_2O \rightarrow 4H^+ + O_2 + 4e^- \qquad (2.2)$$

The oxidation at the Mn-cluster takes place in four steps. This is illustrated in the so called S-cycle, or Kok-cycle (Figure 2.2).[3,4] Each step in the S-cycle is

driven by the photo-excitation and the subsequent oxidation of P680. This means that P680 has to be oxidized and re-reduced by electrons from water at the manganese complex four times to complete one turnover of the cycle. The oxidation power is stored in the manganese cluster in the form of higher Mn oxidation states and probably also as organic radicals coordinated to manganese.[5-7] When the cluster reaches its most oxidized state, a new water molecule comes in and one molecule of oxygen is released.

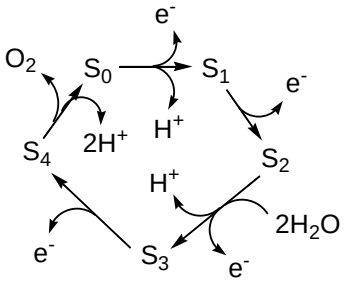

Figure 2.2 The S-cycle for PSII.

2.2 Artificial photosynthesis – aim of the work

Photosynthesis accomplishes storage of energy in the form of biomass, which can be used as an energy source by the organism as well as by mankind. Upon consumption of the energy, water and carbon dioxide is released and available to form new biomass in the next turnover of the cycle (Figure 2.3, left). A similar cycle, also driven by light, but involving other components is the goal in the project of artificial photosynthesis.

The aim is to use the basic principles of PSII to achieve a charge separation by light and to store the energy in a fuel that is more useful than biomass and from which the energy can be extracted with high efficiency. Such a suitable fuel is hydrogen gas. So far the idea has been to mimic the manganese cluster in PSII, *i.e.* to use the absorbed energy in the system for the splitting of water. The products will be electrons and protons that could be used to form H_2. When H_2 is oxidized, for example in fuel cells, the water that was once used to store the energy is reformed. In this way, an environmentally friendly cycle without formation of waste products is available (Figure 2.3, right).

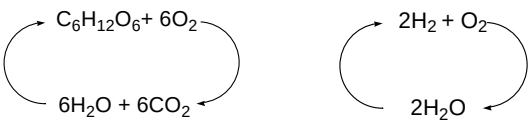

Figure 2.3 A comparison between the coupling of photosynthesis and respiration (left) contra an artificial system for light harvesting and water splitting (right).

In an artificial system, a photosensitizer that mimics the function of P680 in PSII is needed to absorb the energy of the sunlight. Further necessary components are catalytic complexes that perform the water oxidation and the reduction of protons to produce hydrogen. Nature's strategy is to employ many redox components in series. Additional intermediate electron donors and acceptors might therefore be needed also in an artificial system to steer the electron transfer in the desired direction. A schematic structure of such a system is shown in Figure 2.4. The way in which the system might be arranged in order to achieve the highest efficiency is still an unanswered question. A complete functional system with catalytic capacity on both donor and acceptor side has not yet been achieved.

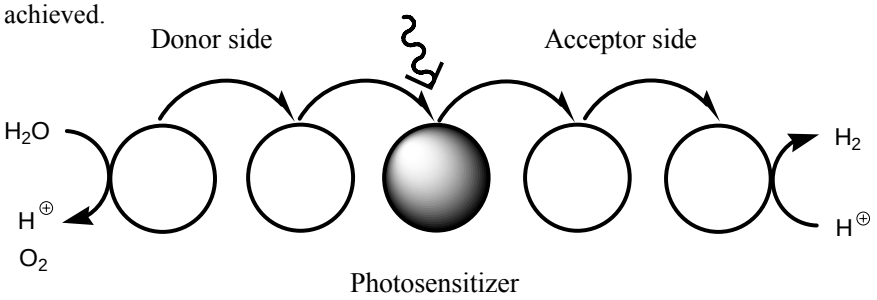

Figure 2.4 Schematic picture of a system for multistep electron transfer and hydrogen production from water. The circles represent redox components. The outer redox components would also have to be catalysts.

Certain components of the system shown in Figure 2.4 have already been studied. For photo-induced electron transfer processes, photosensitizers such as ruthenium-tris-bipyridine and bis-terpyridine complexes have been examined.[8] The photochemical properties of Ru-bipyridine complexes have been known for a long time and are used in different applications. A ruthenium complex is also used in the well established dye-sensitized solar cell, the Grätzel-cell.[9,10]

Mainly manganese complexes have been investigated as potential catalysts for the water oxidation.[11] Unfortunately, only a few synthetic Mn-complexes have been shown to perform water oxidation.[12-14] As the existing information of the structure of the manganese cluster in PSII grows, the possibility to design an appropriate catalyst will increase.

Iron complexes have been studied for the role as proton reduction catalysts, The inspiration for this idea also comes from nature, from enzymes called iron-hydrogenases.[15,16] The research area of proton reduction utilizing iron-complexes is increasing, but so far hydrogen production has only been successfully accomplished electrochemically but not photochemically.[17,18]

Nature uses a tyrosine residue as a redox component between P680 and the Mn-cluster to accomplish an efficient and fast electron transfer. A tyrosine model, *i.e.* a phenol, could thus also be used as an electron transfer mediator in an artificial system. Three main prerequisites are needed to be considered for a phenol for it to be considered to participate in a system for multi-step electron

transfer. First, the phenol should have a suitable redox potential. Secondly, its oxidation has to be fast, and thirdly the formed phenoxyl radical has to be stable enough not to undergo any unwanted chemical reactions during the redox processes. Some models for intramolecular electron transfer using phenols as electron donors in intramolecular complexes have already been presented.[19-23]

Since hydrogen bonding is known to have an important effect on the properties of a phenol, these effects need to be studied in more detail. As a result of this research, it may be possible to design a phenol which can function as a redox switch in our artificial system. This quest has been the aim of this work.

2.3 Hydrogen bonding

Hydrogen bonding is one of the most important non-covalent interactions in biological systems.[24] It is for instance responsible for the association of the two strands of DNA and furthermore crucial for the formation of the secondary and tertiary structure of proteins.

The term hydrogen bond normally refers to a dipole-dipole interaction between an electronegative atom, usually O, N or F, and a proton situated on another electronegative atom. In X_1-H…X_2, with X representing electronegative atoms, the X_1-H compound is called the hydrogen bond donor and X_2 the hydrogen bond acceptor. C-H...X and X-H...φ (where φ is an aromatic system) bonds are also interactions that are considered to be hydrogen bonds. Although they are weaker than the conventional ones they play an important role in chemistry.[25]

There are other types of hydrogen bonds, such as the strong low-barrier hydrogen bonds (LBHB).[26] They are very strong hydrogen bonds that have been proposed to be involved in catalysis and in proton- or hydrogen atom transfer processes in enzymes are called. Another kind of bond is the RAHB (resonance assisted hydrogen bond).[27-29] It is a bond in which the donor and acceptor are linked and conjugated. That gives extra stability to the bond. In this thesis a hydrogen bond refers to a X_1-H...X_2 interaction unless stated otherwise.

By formation of a hydrogen bond the total energy of the system is lowered 1-2 kcal/mol for the weakest ones to up to 40 kcal/mol for the strongest ones. Very strong hydrogen bonds are approaching covalent ones both in strength and character.[30,31]

A small difference in pK_a between the hydrogen bond donor and the corresponding acid of the hydrogen bond acceptor is a requirement for the formation of a strong hydrogen bond.[31] However, even though a system has a ΔpK_a close to 0 a strong bond is not guaranteed. The donor and acceptor abilities of the involved molecules determine how strong the bond will be. Strengths of hydrogen bonds also not only depend on the involved atoms but on the surrounding medium.

With the hydrogen bond distance the distance between the two heteroatoms of the hydrogen bond, X_1…X_2, is meant. It is usually taken as a measure of the hydrogen bond strength, the shorter the distance, the stronger the bond.

Hydrogen bonds often become stronger the more linear they are but exactly

how sensitive the strength is to the angle is depending on the individual hydrogen bond. Among intramolecularly hydrogen bonded systems, six-membered rings are the most favorable ones because a close to linear configuration for the hydrogen bond is possible within the ring.[32] Five-membered rings this are not as favorable geometrically and are therefore less common. Seven-membered rings and larger ones also exist and do not necessarily give weaker hydrogen bonded systems than the six-membered rings since linearity is possible.

To analyze the properties of hydrogen bonds several methods are at hand. One method that gives detailed information on the geometrical parameters in a crystal is X-ray diffraction. It deduces the position of atoms in space from electron density maps and is one of the most powerful methods for studying crystalline materials and also hydrogen bonds in the solid state.

Nuclear magnetic resonance, NMR, is another useful analytical tool. It provides information about the electronic environment of single atoms in a molecule and can be used to analyze compounds in both solid state and in solution. Since hydrogen bonding affects the electronic environment of the participating atoms of a hydrogen bond, NMR analysis can give insight into the character of the bond. The proton involved in a hydrogen bond is very deshielded, and is therefore shifted downfield in a ^{1}H NMR spectrum compared to the corresponding non-hydrogen bonded proton.[33] The most deshielded protons can have chemical shifts down to 16-20 ppm.[31] By using NMR it is sometimes possible to resolve different hydrogen bonds in solution, if those exist. That can be done by decreasing the fast exchange in which the protons are involved by lowering the temperature. Mostly the exchange of the protons between different X-H sites is however fast and only an average response of the different hydrogen bond arrangements can be seen usually resulting in broad peaks. It is also possible to run NMR on other nuclei involved in hydrogen bonding, for example ^{15}N and ^{17}O.

2.3.1 Hydrogen bonding in proteins

In proteins not only the amide functionalities of the peptide backbone and the C- and N-terminal ends of the peptides can participate in hydrogen bonding but also the side-chains of amino acids. The amino acids relevant for this project are tyrosine (**1**), histidine (**2**), glutamic acid (**3**) and aspartic acid (**4**) (Figure 2.5). Their role in proteins will be briefly discussed below.

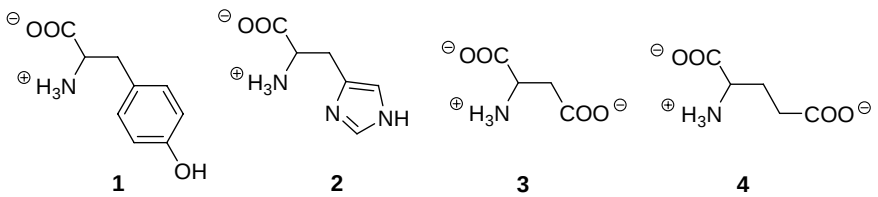

Figure 2.5 The amino acids Tyr, His, Glu and Asp at pH ~6.

The side-chain of tyrosine, Tyr (**1**), contains a phenol moiety which is a better

hydrogen bond donor than acceptor, but both modes are possible. Tyrosine is not only involved in hydrogen bonding but also participates in redox-reactions in many enzymes as for example cytochrome oxidase,[34] galactose oxidase,[35] and RNR (ribonucleotide reductase).[36] It can also act as ligand to metal complexes, either as a phenolate anion or as a phenoxyl radical. Oxidation of phenols will be discussed in chapter 2.5.1.

Histidine, His (**2**), contains an aromatic imidazole moiety, the numbering of which can be found in Figure 2.5. Histidine is often found in active sites of enzymes acting as a ligand for metals. Histidine is normally not participating in electron transfer in proteins but can of course be oxidized if enough potential is applied. There have not been many electrochemical studies on compounds containing imidazole unprotected at the 1-N due to its tendency to deposit on electrodes and to undergo radical polymerization reactions.[37,38]

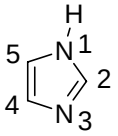

Figure 2.6 IUPAC numbering of the atoms in imidazole.

Biological systems have great for the feature that the pK_a of the protonated imidazole (at the 1-N site) is close to 7. This makes imidazole excellently suited for acting as proton donor or acceptor in acid/base reactions around neutral pH. A small change in environment can substantially change the hydrogen bonding donating or accepting properties.

The amino acids glutamic acid, Glu (**3**), and aspartic acid, Asp (**4**), have carboxylic acid side-chains. They are often involved in hydrogen bonding but also act as ligands for metal complexes. The pK_a-values of the carboxylic acid side chains are ~4 which means that they are deprotonated at neutral pH.[24]

2.4 Quantum chemical calculations on hydrogen bonded systems

The use of computational methods to address chemical problems is increasing rapidly due to development of more powerful computers that give possibilities to develop more accurate methods and programs. Performing calculations to obtain correct information for hydrogen bonded systems is not a trivial task. Hydrogen bonds are much more flexible and more dependent on the surrounding than covalent bonds. This causes problems for comparing experimental results to theoretical ones and vice versa.

For the calculations in this thesis, density functional theory (DFT) has been used. The DFT-methods, that have become very popular in recent years, are not based on determinations of the wave function as the classical *ab initio* methods, but on the electron density of the molecule. This has some advantages but also drawbacks. It makes the DFT-calculations less demanding when it comes to computer power and time as compared to other methods. One drawback with the

present approximations is that London-dispersion forces, *i.e.* van der Waals interactions, are not taken into account. For hydrogen bonds this should not constitute a big problem, since they are dipole-dipole interactions.

For calculations on hydrogen bonded systems, electron correlation has been found to be important to include in the treatment of the system. The simplest way to introduce such effects in calculations is with the *ab initio* method MP2, Møller-Plesset perturbation theory, but it is also introduced in density functionals. It is mainly these two methods, MP2 and different versions of DFT that have been used for calculations on hydrogen bonds.

One type of DFT-methods is the so called hybrid methods that have functionals that contain Hartree-Fock exchange to obtain a better description of the electron density.[39] One of the most used hybrid density functionals is B3LYP.[40] The functional-names are acronyms describing their content. The B3LYP functional can be seen in equation 2.3 where F_x^{Slater} is the Slater exchange, F_x^{HF} is Hartree-Fock exchange,[39] F_X^{Becke} is the gradient part of the exchange functional of Becke, [41] F_c^{LYP} is the correlation functional of Lee, Yang and Parr[42] and F_c^{VWN} is the correlation functional of Vosko, Wilk and Nusair.[43] *A*, *B* and *C* are coefficients determined by Becke[44] using a fit to experimental heats of formation[45] where the correlation functionals of Perdew and Wang[46] were used in the expression instead of F_c^{VWN} and F_c^{LYP}.

$$F_{xc}^{B3LYP} = (1-A)F_x^{Slater} + AF_x^{HF} + BF_x^{Becke} + (1-C)F_c^{VWN} + CF_c^{LYP} \qquad (2.3)$$

The errors in the resulting geometries from structure optimizations with B3LYP, *i.e.* the angles and bond lengths, are usually very small. The medium error in the angles is about 0.62° and the medium error in the bond lengths 0.013 Å.[47] Comparisons of the results of different energies for molecules, obtained from calculations and experiments, have been made on test-batteries of molecules. The mean errors for B3LYP was found to be around 2-4 kcal/mol (including errors for ionization energies, proton affinities and more).[48,49] However, the results are not particularly representative for large molecules, nor for all types of systems and parameters. Hydrogen bonds are also special cases and therefore these estimations do not give much information about the accuracy of the results for hydrogen bonds. It is difficult to tell exactly how large the errors in the calculations really are.

The investigations that have been made of the performance of B3LYP compared to the other functionals for the use on hydrogen bonded systems, have shown that B3LYP is a good compromise between computational cost and accuracy.[50-53] As a general remark on B3LYP it can be said that it is slightly underestimating the hydrogen bond strength systematically compared to the more demanding methods MP2 and coupled-cluster (CC).

In this work, the goal of the calculations has not been to determine absolute values of energies, but more to discover trends. By making comparisons between similar systems, the errors become less troublesome since the same type of errors are probably occurring for similar systems and therefore cancel each other when comparisons are made. Comparisons to experimentally obtained data have

been made to see how well the results correlate and to see if predictions from these kinds of calculations could possibly be made for other systems of similar type.

The choice of basis set can be a crucial factor in the calculations on hydrogen bonded systems. Using smaller basis set in particular can give rise to an error called basis set superposition error (BSSE). When the hydrogen bond donor and acceptor interact, the system will be extra stabilized due to the fact that they can use each others basis set. This lowers the total energy of the system too much when comparing with the two separate parts and therefore results in too high hydrogen bond interaction energies. A way to estimate an upper limit of the BSSE for a particular basis set and system is to determine the counterpoise correction, *CP*. To do that for the hydrogen bonded system A-B, the system is first optimized with a certain basis set. Thereafter, four different single point calculations need to be made. One on only A, taking away B completely, and one on only B with taking away A completely, giving the energies E_A and E_B. Then one on A when exchanging the atoms on B for ghost atoms giving $E_{A+B(ghost)}$, and one on B and exchanging the atoms of A to ghost atoms giving $E_{B+A(ghost)}$. Ghost atoms are empty orbitals that the atoms would have if they existed. The *CP* is then calculated from equation 2.4. The obtained hydrogen bond interaction energy I_{HB} for the system can then be corrected for the *CP*. This is however only an estimation of the error and the accuracy of the procedure has been debated.

$$CP = (E_A + E_B) - (E_{A+B(ghost)} + E_{B+A(ghost)}) \qquad (2.4)$$

The simplest environment to perform calculations in is in vacuum. Vacuum is a very different environment compared to a solution and the errors due to the lack of a proper surrounding can be large. The results should therefore be handled with care. It is possible to add solvent effects by a continuum model, in which the molecule is put inside a cavity in a simulated electric field with a certain dielectric constant ε. The best accuracy is obtained if interacting molecules are modeled explicitly, but since the calculation cost is increasing dramatically when more atoms are added it is not economical to add too many.

In this thesis some radicals have also been subjected to calculations. Open-shell systems are more difficult to obtain good results for than closed-shell systems. The accuracy for B3LYP is lower for radicals, but the same is true for many other methods. For calculating spin-densities of normal phenoxyl radicals it has a performance similar to MP2,[54] but more troublesome systems are the ones in which radicals are engaged in hydrogen bonding. The accuracy has been found to be lower for B3LYP as compared to MP2.[55] The hydrogen bond interaction energies calculated with UB3LYP, were compared to the ones for CCSD (a coupled cluster method). The mean error of B3LYP using full triple zeta basis for a set was similar (3.7 kcal/mol) to the one with for the UCCSD using a small double zeta basis. To obtain very accurate results for hydrogen bonded radicals with B3LYP large basis sets should be used. However, for our calculations the errors do not necessarily have to constitute a problem as long as awareness of them is there. In fact, the results from the calculations conducted by us on hy-

drogen bonded radicals have been shown to correlate well with what was found experimentally (see chapter 6).

For the DFT-calculations in this thesis the program Jaguar 5.5 has been used.[56]

2.5 Redox reactions

Redox reactions are electron transfer reactions between an oxidizing agent, which is reduced, and a reducing agent that is oxidized (eq 2.5). The reaction can be divided into half-reactions that each has their individual reduction potential E_x^0 (eq 2.5 and 2.6). The potentials always have to be referred to a certain reference potential and electrode.

$$D + A \rightarrow D^+ + A^- \qquad E_A^0 - E_D^0 \qquad (2.5)$$

$$D^+ + e^- \rightarrow D \qquad E_A^0 \qquad (2.6)$$

$$A^- + e^- \rightarrow A \qquad E_D^0 \qquad (2.7)$$

The driving force for electron transfer, the standard free energy change of reaction ΔG^0, follows equation 2.8 assuming that electronic repulsion between the species is negligible. F is Faradays constant (96.485 kC/mol^{-1}).

$$\Delta G^0 = -nFE^0 = -nF(E_A^0 - E_D^0) \qquad (2.8)$$

Electron transfer reactions are much faster than nuclear motion. Electrons can only move between orbitals with the same energy, and for this situation to be brought about, reorganization that costs energy is required before the electron transfer can take place. To the total reorganization energy, λ, there are contributions from solvent molecule organization, which is called outer reorganization energy, and an inner one, which is atomic distances and angles etc within the molecules.

2.5.1 Oxidation of phenols and of Tyr_Z in PSII

Phenoxyl radicals have been known since the beginning of the 20th century,[57] and are of interest in many areas of chemistry.

Oxidation of phenols, PhOH, requires high oxidation power because highly energetic phenoxyl radical cations, $PhOH^{\bullet+}$, are formed.[58] A normal phenol is weakly acidic and has a pK_a of ~10,[59] while the formed species $PhOH^{\bullet+}$ is a very strong acid. Determining the exact pK_a-values of phenoxyl radical cations has been attempted, but the information has been difficult to obtain due to the instability of the radical.[58,60,61] Values of less than pK_a 0 can be presumed, but the actual pK_a is probably lower. The high acidity of the formed radical leads to that electron transfer from tyrosine is usually accompanied by deprotonation. This

process of oxidation is called proton coupled electron transfer, PCET.[62,63]

If the phenol is engaged in hydrogen bonding prior to the oxidation, the redox potential can be lowered. Fang *et al.* studied the impact of hydrogen bonding to different amines on oxidation of phenol and found a linear correlation between the basicity of the amines and the potential for the oxidation, showing that it is not the hydrogen bond strength that is important for the redox properties of the phenol but the proton accepting properties of the base. The same thing was observed by Linschitz and coworkers when analyzing the rate of oxidation of phenols forming intermolecular hydrogen bonded complexes to pyridines in solution.[64] However, what the exact reason is for the lowering of the reduction potential by the proton acceptor still remains to be elucidated.

Although the kinetics of phenol oxidation is also altered by hydrogen bonding also, not many studies on the subject have been performed. One of the few examples is a tyrosine covalently linked to ruthenium(II) trisbipyridine. Upon attachment of dpa-arms (dipicolylamine) to both *ortho*-positions of the tyrosine, it could be oxidized much faster intramolecularly by Ru(III).[23]

Phenoxyl radicals are well known examples of stable radicals, provided that the *ortho*- and *para*-positions are substituted to prevent radical coupling reactions; the bulkier substituents, the better. One example of a persistent radical is the 2,4,6-tri-*tert*-butyl phenol that can be stable for days in carbontetrachloride.[57] The sterical hindrance provides so called kinetical stability, in contrast to thermodynamical stability which depends for example on hybridization or mesomerism.[65]

One way to obtain information about the redox properties of a compound is to use cyclic voltammetry, CV. In CV an electrical potential is applied to a solution and is varied in a cyclic manner, from low potentials to high and back again (or the opposite depending on what is supposed to be studied) An electric current is observed at the reduction potential of the compound and an electric current is observed in the opposite direction for the corresponding reduction of the species when the potential is decreased again, that is if the reaction is reversible. Reversibility of a process is a sign of stability of the involved species and for a fully reversible reaction the oxidation and reduction waves must be of the same magnitude.

Most phenols can not be oxidized and reduced reversibly, only deprotonated phenols can be due to their lack of protons.[66] The reversibility in CV is also dependent on the scan-rate used. Many phenols can actually be reversibly oxidized by using fast voltammetry with scan-rates between 5000-50 000 V/s.[67]

A related electrochemical technique is differential pulse voltammetry, DPV. In DPV the potential is pulsed instead of scanned as in CV, but the resulting voltammograms looks like a CV-spectra being run in only one direction. DPV gives a better resolution and is therefore superior to CV when processes occurring at similar potentials are to be studied.

The presence of hydrogen bonding to a phenoxyl radical can improve its stability and make its formation (oxidation) and reduction more reversible. Maki *et al.* was the first to present a reversible oxidation of a phenol due to hydrogen bonding to a proton acceptor.[68] This was accomplished with a phenol linked to a

tertiary amine that could form an intermolecular hydrogen bond to the phenol. The mechanism was proposed be one a "proton rocking mechanism", in which the proton is abstracted upon oxidation and returned upon reduction.

Scheme 2.1 "The rocking proton mechanism".

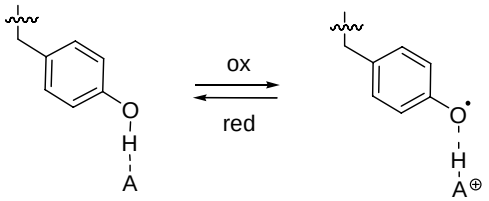

In a phenoxyl radical, the spin is delocalized over the ring, in an odd-alternate fashion.[69] The radical absorbs light in the visual part of the spectrum and can therefore be studied by UV-VIS spectroscopy. A broad absorption around 600 nm is usually accompanied by some stronger ones at wavelengths around 400 nm.[70]

Transfer of the proton of tyrosine in addition to the electron transfer is required energetically for the oxidation of Tyr_z to occur. This has now been shown by many groups, both for model systems and for photosystem II.[38,71-73] The result of the oxidation is a neutral tyrosyl radical, probably being hydrogen bonded, either to the protonated base or to another hydrogen bond donor. Upon reduction of the radical the phenol becomes protonated again.

There is, however, no agreement on the exact on the mechanism for oxidation/reduction of Tyr_Z during the cycle of the enzyme, for example on the faith of the abstracted proton. It could either stay on the immediate proton acceptor or in the vicinity on another proton acceptor,[74] Another proposal is that it is transferred to the bulk and a new proton originating from water is transferred there from the manganese complex.[75,76]

Furthermore, since both electron and proton transfer is involved, there are different possible mechanisms with which the oxidation (and reduction) can occur (Scheme 2.2). Proton transfer, PT, can take place before, after or at the same time as the electron transfer, ET. The different pathways have different thermodynamic characteristics and can work in parallel for the phenols in solution.

Scheme 2.2 Different pathways for oxidation of a phenol.

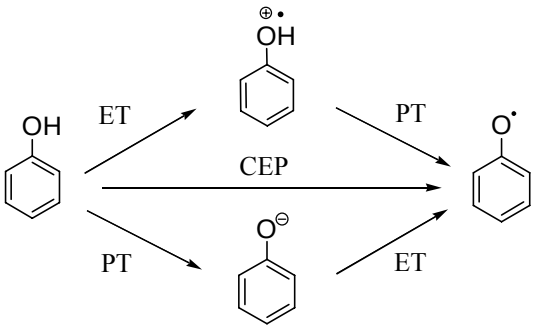

Electron transfer reactions are highly dependent on the properties of the surrounding medium in which they occur. In water, PCET-reactions can only take place in the pH-interval between pH=$pK_a(PhOH^{\bullet+})$ and pH=$pK_a(PhOH)$. The energetics of the PCET-reactions for oxidation of phenol in water can be rationalized in schemes such as the one depicted in Figure 2.7. The horizontal line represents the reduction potential E^0 of a fictive oxidant to which electron transfer from the phenol would occur, and the graph shows the potential for oxidation of an ideal phenol that would strictly behave according to the $pK_a(PhOH^{\bullet+})$ and $pK_a(PhOH)$ values. The vertical arrows show the driving forces for the electron transfer steps in ETPT (1) (which in this case would be endergonic), and the driving force for CEP (2, ender- or exergonic dependent on the pH) and the one for the electron transfer step in PTET (3, which is exergonic). Electron transfer from a phenolate is not a PCET reaction and is not described by Figure 2.7, but the driving forces for electron transfer from a phenolate and for the electron transfer step in the PTET-mechanism are the same.

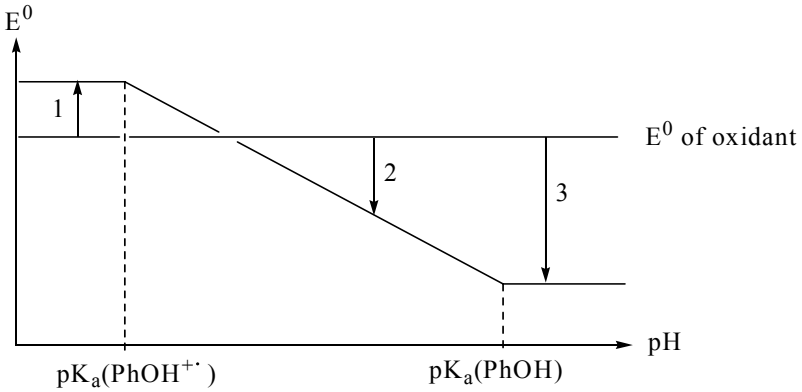

Figure 2.7 Energetics of an electron transfer reaction between a phenol and an oxidant.

If proton transfer takes place after the oxidation, an ETPT-mechanism would occur. The electron transfer is likely to be the rate determining step since the reaction is endergonic. This reaction step involves no protons, and the over-all rate for the mechanism will be independent of pH. Because a pure electron transfer determines the rate, the reorganization energy is usually small. The reduction potential for an ETPT-reaction is the one that can be seen at a pH below $pK_a(PhOH^{\bullet+})$, but in reality the proton of the radical cation will not leave, since protonated radical is stable at those low pH-values.

The second possibility is that the proton leaves at the same time as the electron. This leads to a concerted reaction, abbreviated CEP. For the CEP-mechanism there can only be one single transition state. This means that the electron transfer has to take place at the same time as the proton transfer, but the two do not need to go in the same direction. The driving force for a CEP-

reaction is pH-dependent, which is seen in Figure 2.7. The pH-dependence (with a slope of 59 mV/pH) derives from the fact that the released protons have different energies of mixing depending on the pH, *i.e.* it is more favorable to release protons to a solution with a high pH instead of a low. This affects the redox potential for $PhO^{\bullet}$/PhOH, which determines the driving force of the reaction, $\Delta G°$. The higher the pH becomes, the higher the driving force will be. The CEP-mechanism is believed to have high reorganization energy λ because the O-H bond has to be distorted in the process to enable the electron transfer.

The third case is if the proton leaves the phenol before the electron transfer takes place, the PTET-mechanism. The driving force for the electron transfer reaction in this mechanism is the one shown by arrow 3 at high pH; a phenoxide ion is much easier to oxidize than a protonated phenol and the rate constant for the electron transfer is also higher.

After the proposal of the importance of hydrogen bonding for oxidation of Tyr_Z in PSII, evidence started to accumulate for that a histidine residue, His190, was the immediate proton acceptor of Tyr_Z.[77-83] In one interesting study for example, His190 was mutated away, which dramatically decreased the enzyme function. The activity, however, could be restored by addition of small bases, for example imidazole, that was believed to take the place and function of His190.[80] However, the X-ray structures of PSII have disagreed on whether the distance between His190 and Tyr_Z is short enough for a strong hydrogen bond interaction.[2,84-86] According to experiments, the environment around Tyr_z is highly disordered and a large hydrogen bonded network, including solvent molecules *i.e.* water, are likely to be involved in the proton transfer and redox events. This is supported by the fact that the site is accessible to solvent.[81] According to the X-ray structure of PSII with the best resolution so far, 3.0 Å, the two closest positioned amino acids to the hydroxyl group of Tyr_z besides His190 are Glu189 and Gln165 of the D1-protein (Figure 2.8). The separation of the Tyr_Z oxygen atom and the closest imidazole nitrogen atom in His190 is 2.77 Å.

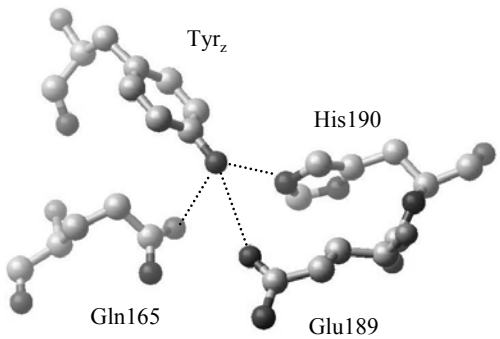

Figure 2.8 The site around Tyr_Z with the three closest lying amino acids.[2]

Another tyrosine residue, Tyr_D or Y_D, is redox-active in PSII and form a hydrogen bond to a histidine residue, His189 of the D2-protein (see ref 87 and

references therein). Even though both tyrosine residues have hydrogen bonds to the same kind of amino acid, their characteristics are different. Tyr_D seems to be involved in a simpler hydrogen bonded network than Tyr_Z. The site is also less solvent accessible and the rate by which it is oxidized is lower than for Tyr_z. Tyr_Z is oxidized on a sub microsecond timescale and Tyr_D on a second timescale. Tyr_D is not involved directly in water oxidation but might play an indirect role for it.[88]

2.5.2 $[Ru(bpy)_3]^{2+}$ as a photosensitizer

Ruthenium(II) trisbipyridine, $[Ru(bpy)_3]^{2+}$, is a well studied metal complex that has been widely used in systems for photo-induced electron transfer.[8,89] From a chemical point of view, it is a very stable complex in which the ligand-metal bonds are rather insensitive to a variety of reaction conditions, making the complex relatively easy to handle and easy to modify. The reduction potential of the redox couple $[Ru(bpy)_3]^{3+/2+}$ is 1.26 V vs. NHE,[89] which is close to that of P680 in PSII (1.12 V vs. NHE[75])

In solution the ruthenium complex appears red, and its absorption spectrum in the visual region is dominated by an absorption at a λ_{max} of 452 nm with an extinction coefficient, ε_{452}, of 14600 $M^{-1}cm^{-1}$ (Figure 2.11).[89] This excitation corresponds to a t_{2g} to π_L* transition and results in a metal to ligand charge transfer singlet state, ^{1}MLCT. The ^{1}MLCT-state is very short-lived and undergoes intersystem crossing to the triplet state, ^{3}MLCT. The triplet state is more stable with an excited state lifetime τ of 0.9 μs in acetonitrile solution.[8,89]

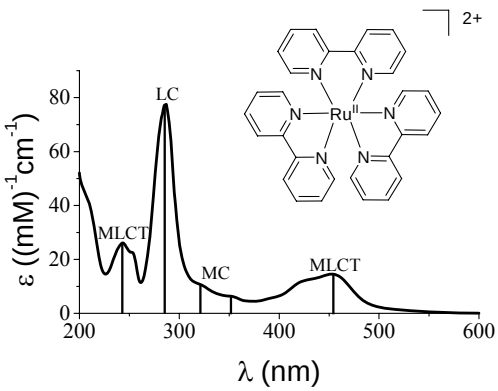

Figure 2.8 Absorption spectrum of $[Ru(bpy)_3]^{2+}$.

The ^{3}MLCT excited state can structurally be described as $[Ru^{III}(bpy)_2(bpy^{\bullet-})]^{2+}$, and can both act as an oxidant and as a reductant. These processes are called reductive and oxidative quenching, respectively. The oxidative quenching (eq 2.9) generates $[Ru(bpy)_3]^{3+}$ that can be used as an oxidant for a molecule M (eq. 2.10).

$$[Ru(bpy)_3]^{2+*} + A \rightarrow [Ru(bpy)_3]^{3+} + A^- \quad (2.9)$$

$$[Ru(bpy)_3]^{3+} + D \rightarrow [Ru(bpy)_3]^{2+} + D^+ \quad (2.10)$$

In the work described in this thesis, laser flash photolysis has been used to generate Ru(III) to be used as an oxidant for phenols (acting as D in eq. 2.10). A laser pulse at 450 nm excites Ru(II), and Ru(III) is generated as described above. The electron acceptor A in equation 2.9 has been methyl viologen (MV^{2+}, Figure 2.10) in the measurements that will be presented. A radical, $MV^{\bullet+}$, is formed upon its reduction. The quenching rate by MV^{2+} is diffusion controlled with a rate constant of $5.6 \cdot 10^9$ $M^{-1}s^{-1}$.[8] This value sets an upper limit for the highest reaction rates that can be studied with this method. The recombination between $MV^{\bullet+}$ and Ru(III) then sets a lower limit for the slowest reactions.

The electron transfer events can be followed by the bleach (decreased relative absorbance compared to the starting state: Ru(II)) at 450 nm due to the generation of Ru(III) according to the reaction in eq. 2.9. The back reaction between Ru(III) and $MV^{\bullet+}$, and later between the oxidized tyrosine and $MV^{\bullet+}$, can also be followed at the characteristic absorption for $MV^{\bullet+}$ around 600 nm. The rates of electron transfer to the Ru(III) from the donor can be extracted from the kinetic traces.

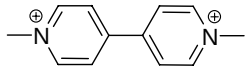

5

Figure 2.9 Methyl viologen, MV^{2+}.

3 Calculations on hydrogen bonded phenol-amine systems

Since it is known that a histidine residue is very important for the function of PSII and probably acts as a proton acceptor of Tyr_Z, we wanted to study the hydrogen bond interaction between phenol and imidazole in more detail. Not many studies have so far been devoted to hydrogen bonded phenol-imidazole systems. Calculations have shown the impact of hydrogen bonding of imidazole to phenols on the phenol redox properties and phenol-imidazole models to which more hydrogen bonding molecules have been introduced to form hydrogen bonded chains have been studied.[73,90-92]

What are usually studied by means of calculations are optimal systems in which the hydrogen bonds take on their best possible values, with vacuum being the most common environment to perform the calculations in. In a more realistic environment, as within proteins and solution, the hydrogen bonds are altered by their surrounding in many ways which can have a dramatic effect on their properties.

To expand the existing knowledge for this particular hydrogen bond, two different studies were made that have in common that they deal with the sensitivity of the bond to unfavorable steric conditions. In chapter 3.1 the results of an investigation of an intermolecularly hydrogen bonded phenol-imidazole system will be discussed. The following chapter, 3.2, deals with intramolecularly hydrogen bonded systems containing different amines, in addition to imidazole. The results from the calculations have been part of the background work for the synthesis and studies of the compounds in chapter 6.1.

3.1 Intermolecular hydrogen bonding between phenol and imidazole

To investigate how the phenol-imidazole hydrogen bond would be affected by strain, geometrical constraints were put on the optimization of a chosen model system, consisting of a phenol forming an O-H...N hydrogen bond to imidazole.

The choice of basis set for the calculations was made from a basis set investigation (Table 3.1). I_{HB} is the hydrogen bond interaction energy calculated as the difference in energy between the optimized hydrogen bonded system and the sum of the separately optimized hydrogen bond donor and acceptor. The results showed that the basis set 6-31+G* (a double zeta basis set with one set of polarization functions and one set of diffuse functions on all atoms except hydrogen) had a low BSSE (see chapter 2.4). This basis set has been found by others to be a good choice for hydrogen bonded systems and is believed to even out two factors: the too low binding energies usually obtained with DFT, and the too high binding energies obtained with the use of a small basis set (Unpublished results Marco Bocola).

Table 3.1 Results from optimizations of a hydrogen bonded phenol-imidazole system using different basis set.

Basis set	O-H (Å)	N...H (Å)	O...N (Å)	O-H...N (°)	BSSE (kcal/mol)	I_{HB}[a] (kcal/mol)
6-31G	1.007	1.735	2.740	175.49	-1.570	14.249
6-31G*	0.989	1.866	2.853	175.95		
6-31G**	0.987	1.838	2.824	175.74		
6-31+G	1.009	1.729	2.735	175.22		
6-31++G	1.009	1.728	2.734	175.43		
6-31+G*	0.990	1.860	2.848	175.09	-0.914	9.912
6-311G	1.001	1.731	2.735	172.67		
6-311G**	0.984	1.842	2.822	174.02	-2.216	11.190
6-311+G	1.003	1.737	2.739	175.53		
6-311++G	1.003	1.736	2.737	175.43		
6-311+G*	0.984	1.866	2.846	173.96		
6-311++G**	0.985	1.850	2.832	173.95		

[a]BSSE-uncorrected I_{HB}.

The O…N distance was frozen to different values and the system was optimized at each distance (Figure 3.1). The position of the proton was not fixed, which resulted in different angles for the different O…N distances (Figure 3.2).

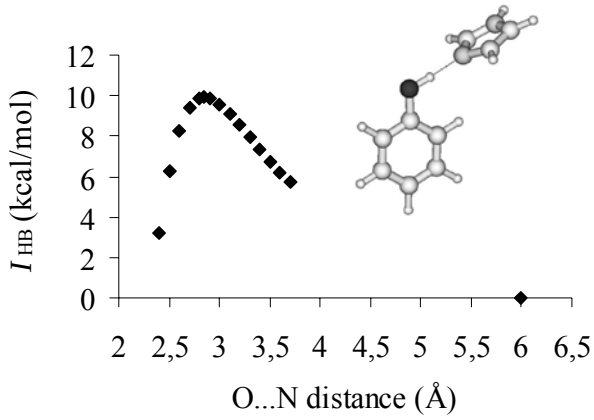

Figure 3.1 The dependence of the I_{HB} on the O…N distance for the shown structure.

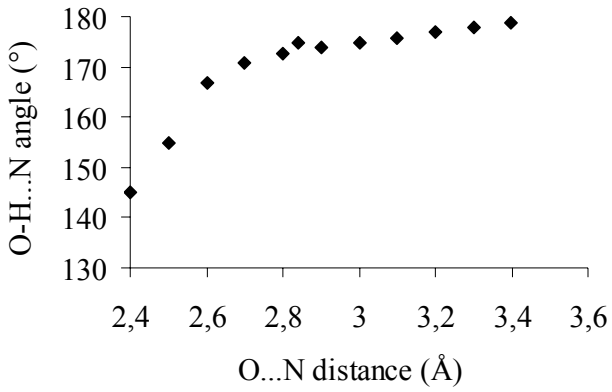

Figure 3.2 The dependence of the hydrogen bond angle O-H…N on the O…N distance for the phenol-imidazole model in Fig. 3.1.

In the diagrams in Figure 3.1 and 3.2 it can be seen that I_{HB} is not very sensitive to small variations in the geometry. At such a large distance as 3.5 Å there is still some interaction left between the hydrogen bond donor and the acceptor. This might be of relevance for PSII, for which some X-ray structures have shown a separation between Tyr_Z and His190 of more than 3.5 Å. The results show that even at longer distances than the ones considered being normal for the O-H…N hydrogen bonds (2.6-3.0 Å), there can be significant communication between the hydrogen bond donor and the acceptor. The communication between the two could possibly also be preserved via a water molecule (as will be discussed in chapter 4.3).

At smaller O…N distances than the optimal ones, the imidazole ring moved to the side of the phenol, but the torsion angle C-C-O-H was kept at around 0° degrees resulting in a more bent angle O-H…N angle. The angle approached 180° when the O…N distance was increased, since the interaction becomes more electrostatic.

It seemed to be important to keep the torsion angle C-C-O-H low for the phenol. Therefore hydrogen bond for the phenol-imidazole system was frozen to different values and optimization of all other parameters of the system was made. The energy for the hydrogen bonded system increased gradually with a larger torsion angle, and at an angle of 90° it had increased by 3.9 kcal/mol compared to the optimal system with a torsion angle of 0°. For a phenol without hydrogen bonding the energy increased by 3.5 kcal/mol by rotating the O-H 90° out of the phenol plane. The resulting structures had the imidazole rotated, to a different extent depending on the torsion angle (Figure 3.3). This lowers the energies for the systems slightly, but the interaction is probably weak. The parameters for the hydrogen bond geometries were essentially the same at all torsion angles.

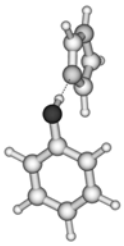

Figure 3.3 The structure of the phenol-imidazole model at a C-C-O-H torsion angle of 90°.

Two types of interaction energies were considered at the different torsion angles. One was calculated as the difference between the energy for the hydrogen bonded system at that particular torsion angle and the sum of energies of freely optimized phenol and imidazole (dots in Figure 3.4). Another was the difference between the energy for the hydrogen bonded system at a particular torsion and the sum of the energy of the phenol with that particular torsion angle plus the energy for optimized imidazole (triangles in Figure 3.4). The values of the I_{HB} showed that hydrogen bonding to imidazole lowers the energy of the system by about the same amount at every torsion angle. If the hydroxyl group is rotated out of the plane, the conformation of the system becomes energetically unfavorable for the system. However the effect of the imidazole was shown to be of similar size irrespective of the torsion angle.

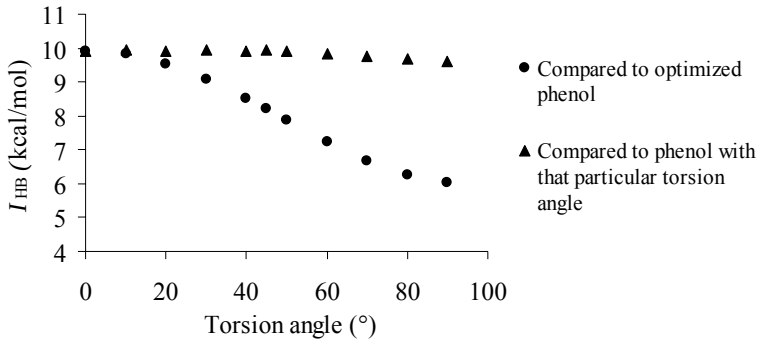

Figure 3.4 The dependence of the I_{HB} on the torsion angle C-C-O-H for phenol of the model in Fig. 3.1.

3.2 Intra-molecular systems

To optimize the possibilities for strong hydrogen bonding, a good choice is to have the hydrogen bond donor and acceptor linked to each other. The studies for systems with intramolecular hydrogen bonds between phenol and imidazole so far have been focused on imidazole units coupled directly to the phenol ring resulting in resonance assisted hydrogen bonds.[94-96] These structures are not representing the situation in proteins well because the tyrosine and the histidine are not in conjugation but are sitting on different amino acids. The aim with the performed calculations was to compare some already existing intramolecularly

hydrogen bonded phenols to some new ones that might be worth synthesizing and study experimentally.

For geometry optimization of the models a small basis set 6-31G (a double zeta basis) was used and determination of the energy for the structures was made with the larger basis set 6-311G** (a triple zeta basis with polarisation functions on all atoms). In Table 3.2 and 3.3 the results for the different models are summarized.

Table 3.2 The intermolecularly hydrogen bonded models **I-IV**.

		I_{HB} (kcal/mol)	IP (kcal/mol)	O…N (Å)	ΛO-H…H (°)
I	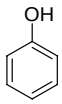	-	193.9	-	-
II	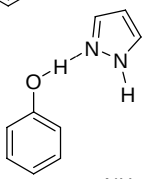	9.1	162.3	2.77	162.1
III	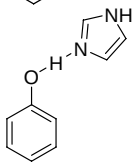	9.7	155.7	2.74	175.5
IV	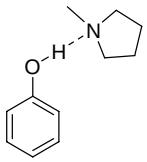	10.5	151.4	2.68	166.6

Upon oxidation of all studied models the protons are transferred to the amines automatically. The ionization potentials IP for the models **II-IV** are following the trend that is expected considering the basicity of the amines (the pK_a values of their corresponding acids are ~10, 7 and ~3, respectively), the stronger the base the lower the IP.[92] Their I_{HB} are similar but are also following the same trend.

Table 3.3 The intramolecularly hydrogen bonded models.

		I_{HB} (kcal/mol)	IP (kcal/mol)	O…N (Å)	ΛO-H…H (°)
V	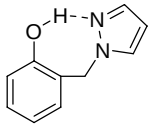	6.0	167.8	2.70	159.6
VI	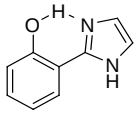	15.1	165.0	2.58	145.8
VII	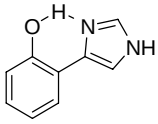	13.8	163.7	2.60	145.9
VIII	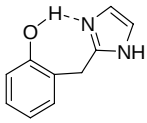	9.1	157.9	2.66	160.1
IX	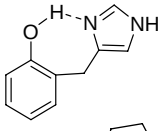	7.1	157.9	2.68	160.0
X	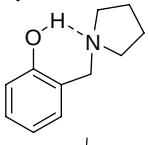	7.8	158.6	2.65	148.4
XI	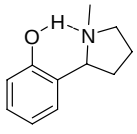	9.8	159.9	2.67	148.2

The calculations showed that an imidazol-2-yl-group linked via a methylene-bridge to the *ortho*-position of the phenol (model **VIII**) would give a similar hydrogen bond strength and geometry as an optimal hydrogen bond between imidazole and phenol (model **III**). The methylene-linker keeps the hydrogen bond acceptor and donor sufficiently close to each other without allowing too much flexibility. It also interrupts the conjugation (in contrast to models **VI** and **VII** have) between the two, so the parts will act nearly individually. The largest difference between model **VIII** and the optimal model **III** is the smaller hydrogen bond angle (160° compared to 175.5°), but the results presented in the previous chapter suggest that there is considerable flexibility in the bond. That the differences in the angles do not play a great role is therefore not surprising. Fur-

thermore, the O-H in model **VIII** is also turned 30° out of the plane compared to the intermolecular model **III** (see paper IV for more information on the hydrogen bond geometries), but this too does not seem to play a significant role for the hydrogen bond.

Models **VI** and **VII** have the strongest intramolecular hydrogen bonds. That is due to that the fact that they are resonance assisted (RAHB). The two aromatic rings lie in the same plane to maximize the conjugation of their π-overlap and thereby the hydrogen bond strength. The results show that these two structures probably do not well model the situation for Tyr_Z and His190 in PSII. The arrangement in PSII is almost certainly better represented by the intermolecular model **III**.

Compounds with the structures of **X** and **XI** have been studied experimentally.[68,97] The two were found to have very similar oxidation potentials, which is consistent with our calculated results. However, the I_{HB} value of **X** was 2 kcal/mol lower than that of **XI**. The reason for this is not clear, but it could be due to more strain in the model **X** than for the other, **XI**. The optimization of model **X** was also difficult to converge. It was the only optimization that experienced such a problem.

The hydrogen bonds in intramolecular systems will always be a little weaker in strength, or of similar strength, as the optimal intermolecular bond (depending of course of the exact arrangement in the systems). A general conclusion that can be drawn from these calculations is that the methylene linked models rather well model the hydrogen bonds in the intermolecular systems.

3.3 Conclusions

The calculations suggest that the phenol-imidazole hydrogen bond is quite insensitive to the exact O-H…N hydrogen bond geometries.

The strategy of linking an amine and a phenol seems to be a good way to obtain strong hydrogen bonds between the phenol and the hydrogen bond acceptor, even if a seven-membered ring is formed. A structure with a good intramolecular hydrogen bond between phenol and imidazole (**VII**) was found that mimic an optimally hydrogen bonded system well.

4 Hydrogen bonded solid-state structures

Even if the resolution of the X-ray structures of PSII will increase, not much more information might become available on the exact arrangement of the amino acids in the vicinity of Tyr_Z. Studying hydrogen bonds in proteins using X-ray diffraction is problematic for two reasons. First, the substantial mobility of the atoms in proteins due to thermal motions results in that crystallized proteins more behave as gels than hard solids. Crystallized enzymes sometimes even maintain their activity. It has been shown that crystallized PSII evolve oxygen, *i.e.* it can still perform catalysis in this form.[98] Secondly, hydrogen atoms have the lowest electron density of all atoms. Their positions are therefore the hardest to determine. As a result, not many X-ray structures of proteins contain the position of the hydrogen atoms. Structural information from smaller model systems, whose structures are easier to determine by X-ray diffraction, might be of help in studying the structure and function of the larger and more flexible enzyme systems.

It was discovered that compounds **10**-**13** (Scheme 4.1) formed O-H…N hydrogen bonds in the solid-state between phenol and imidazole. All compounds showed broad IR-absorptions between 3300-2200 cm^{-1}, analyzed as KBr-tablets. The broadness of the absorptions, their displacement towards shorter wavenumbers and the lack of the sharp peak for the O-H, usually around 3400-3500 cm^{-1}, were clear indications of that strong hydrogen bonding being involved. Figure 4.2 shows a representative IR-spectrum.

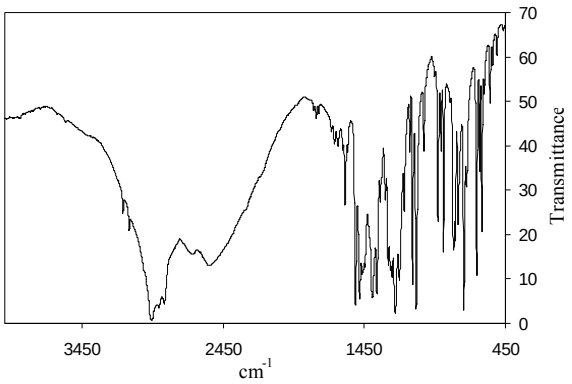

Figure 4.1 IR-spectrum of **12** as KBr-tablet.

To learn exactly what hydrogen bond patterns gave rise to these peaks, the solid-state structures of **10**-**13** were determined by X-ray diffraction, and the compounds were also analyzed with solid-state NMR. **13** proved to incorporate water into the structure, resulting in a hydrogen bonded network much resem-

bling a protein-structure. It will be discussed in chapter 4.3. Compounds **10-12** are discussed in chapter 4.2.

4.1 Synthesis

The synthesis of compounds **10-13** was carried out smoothly by melting the corresponding benzyl alcohols with five equivalents of imidazole.[99] The reaction proceeds via an *o*-methylenequinone intermediate (Scheme 4.1). To obtain the symmetrical phenol **13** the benzyl alcohol **9** was used as starting material.

Scheme 4.1

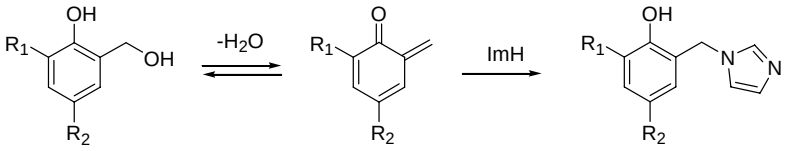

6 R_1=H, R_2= H
7 R_1=Me, R_2= Me
8 R_1=*t*-Bu, R_2= *t*-Bu
9 R_1=hydroxymethyl R_2= Me

10 R_1=H, R_2= H
11 R_1=Me, R_2= Me
12 R_1=*t*-Bu, R_2= *t*-Bu
13 R_1=methyl-imidazol-1-yl R_2= Me

In addition, the ^{15}N enriched versions of compounds **10-12** were synthesized to increase the sensitivity of the ^{15}N NMR experiments (see below). The synthesis was accomplished by preparing ^{15}N enriched imidazole from formaldehyde, glyoxal and ^{15}N labeled (to 60-80%) NH_4Cl, which subsequently was used in the reaction described above.[100]

4.2 Phenol and imidazole

Compounds **10-12** were found to have O-H…N hydrogen bonds between the 3-N atom of imidazole and the hydroxyl group of phenol, although the structural arrangements of the molecules in space were different in all cases due to their different substituents. Since we had a series of compounds with hydrogen bonding between the same hydrogen bond donor and acceptor resulting in different structures, we saw an opportunity of comparing the formed hydrogen bonds and study what might determine the overall structure.

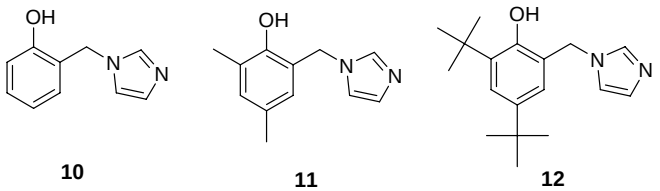

Figure 4.2 The phenols investigated in the solid state.

By examining the resulting three-dimensional structures of **10-12** (Figure 4.3) and the geometrical parameters of the hydrogen bonds (Table 4.1), we concluded that the bond in compound **10** best resembled an optimal bond between phenol and imidazole. The hydrogen bond parameters were also very similar to the ones for Tyr_Z and His190, as revealed by the X-ray structure of PSII with the highest resolution so far.[2]

The absence of sterical hindrance in one *ortho*-position gave **10** the possibility to keep the O-H in the phenol plane resulting in a torsion angle of only 11° (the optimal angle is 0°). As a result **10** was formed a straight chain-arrangement so the two aromatic planes could be close to perpendicular to each other, as for an optimal bond.

Accordingly, the sterical hindrance of the *tert*-butyl group in the *ortho*-position of **12** prevented a chain-like arrangement, leaving the only possibility to form a hydrogen bond to imidazole by adopting a high C-C-O-H torsion angle (62°), which resulted in the formation of dimers. The stability of the dimer-structure was also favored by the *p-tert*-butyl groups pointing outwards the dimers, and the whole crystal was thereby divided into hydrophobic regions and hydrophilic region, containing the *tert*-butyl groups and the hydrogen bonds, respectively.

The structure of **11**, which was found to contain two independent molecules in the unit cell (denoted **11a** and **11b**), had in intermediate situation by having not as large alkyl substituents as **12**. The compromise between **10** and **12** turned out to be a chain-like arrangement, but a more twisted one than for **10.** The sterical hindrance in **10-12** is reflected clearly in the torsion angel C-C-O-H of the compounds, with the smallest one for **10** and the largest one for **12**.

10

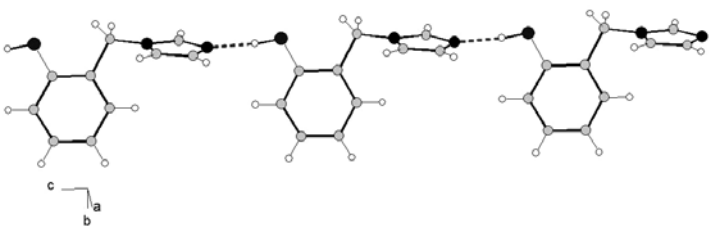

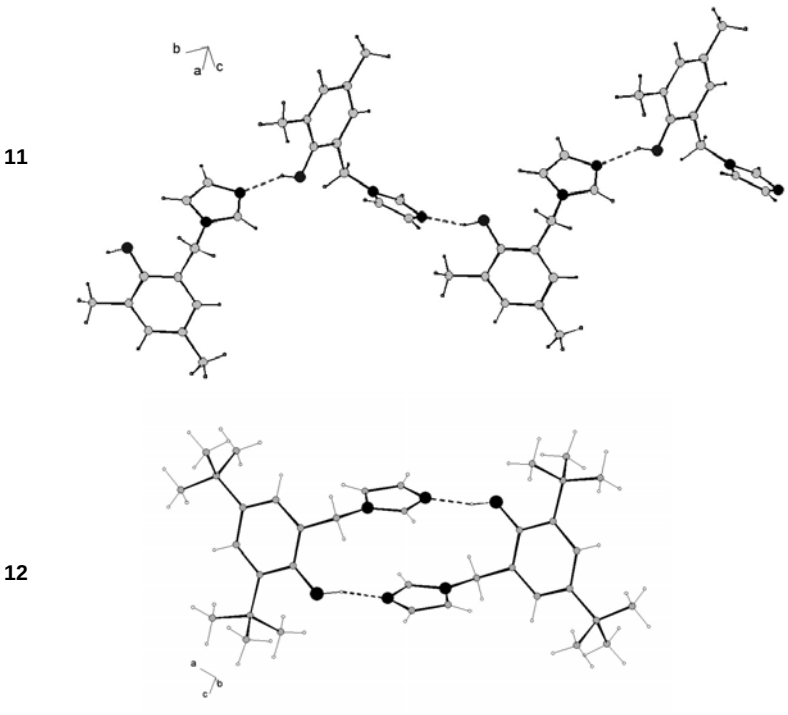

Figure 4.3 Structure fragments of compounds **10-12**.

Table 4.1 Hydrogen bond geometries for **10-12.**

Compound	O-H (Å)	H...N (Å)	O...N (Å)	ΛO-H…N (°)	O-H out of phenol plane (°)
10	0.99	1.90	2.718	174	11
11a	1.01	1.70	2.671	161	33
11b	1.00	1.73	2.700	164	24
12	0.94	1.73	2.656	168	62

The solid-state ^{1}H MAS NMR measurements supported the conclusions from the examination of the structures of **10-12**. The chemical shifts for the hydroxyl proton were determined to 13.2 ppm for **10**, 11.5 ppm for **11** and 11.7 ppm for **12** (the peak for the methyl protons for **11** was set to 1 ppm). These values can therefore be interpreted as **10** has the strongest hydrogen bond.

Upon stronger hydrogen bonding, an upfield shift of the ^{15}N resonance of the participating nitrogen atom is expected.[101,102] However, the ^{15}N NMR spectra showed only small differences in chemical shifts for the hydrogen bonding nitrogen atoms (those at higher chemical shifts) of **10-12** (Figure 4.4). A slightly

lower shift was observed for **10** than for **11** and **12**, but the differences were too small to be assigned unequivocally to stronger hydrogen bonding. There was, however, a quite large upfield shift of the 1-N peak of **10** compared to **11** and **12**. This we believe is due to crystal packing effects. ^{1}H NMR seems to be a better technique to use for these particular compounds for probing the hydrogen bonds than ^{15}N NMR.

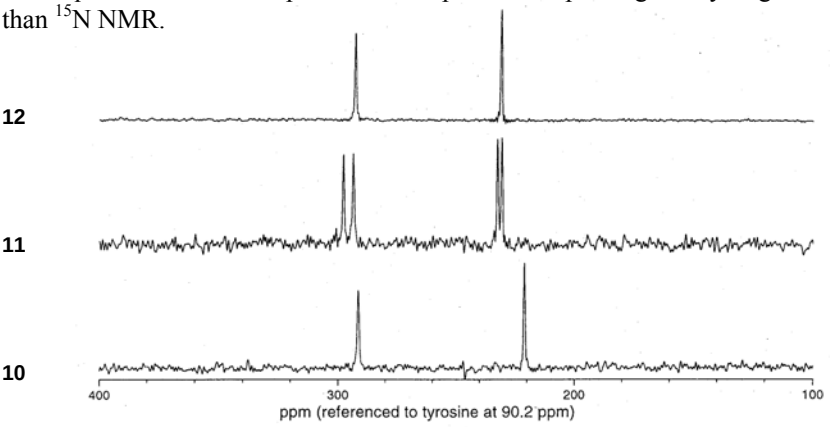

Figure 4.4 ^{15}N CP-MAS NMR spectra of **10**-**12**.

^{13}C NMR was applied to **10**-**12** to see if an effect of the different hydrogen bonds could be seen on the carbon atom closest to the hydrogen bond site, *i.e.* the C-O of the phenol (Figure 4.5). A higher chemical shift of C-O (the peaks most downfield) is expected upon stronger hydrogen bonding, since the bond would get more double bond character. Indeed a difference between the positions of the *C*-O peaks was found for the compounds, but by comparing with existing literature data we concluded that the differences were too small to be assigned to a difference in hydrogen bonding.[103]

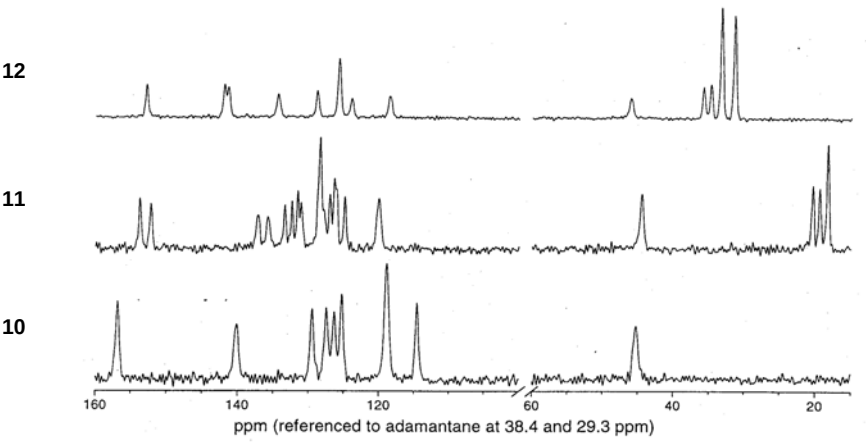

Figure 4.5 ^{13}C CP-MAS NMR spectra of **10**-**12**.

To exclude that the differences seen in ^{1}H NMR were the result of only an electronic effect by the substituents, we wished to compare the compounds in the absence of hydrogen bonding. Unfortunately, dissolving the compounds, especially **10** and **11,** turned out to be difficult in non-hydrogen bonding solvent. They were however, soluble in *d6*-DMSO, which is a weakly hydrogen bond accepting solvent. The most relevant ^{1}H, ^{13}C and ^{15}N chemical shifts of compounds **10-12** in *d6*-DMSO are listed in Table 4.2. As in the solid state there is a possibility for the compounds to form intermolecular O-H…N hydrogen bonds. If that is the case, it would be seen as concentration dependence on the chemical shifts, thus measurements were made at two different concentrations, 0.1 M and 1 M. Such an effect could indeed be seen in the ^{1}H NMR results for **10**. The shift increased with 0.5 ppm by going to higher concentration.

Table 4.2 Chemical shifts δ in ppm of **10-13** in *d6*-DMSO.

Compound	Conc (M)	^{1}H-NMR of O-*H*	^{13}C-NMR *C*-OH	^{15}N-NMR[a,b] 1-N	^{15}N-NMR[a,b] 3-N[c]
10	0.1	9.80	155.64	-	-
	1	10.29	155.85	112.75	197.10[c]
11	0.1	8.49	151.05	-	-
	~1[d]	8.41[c]	151.17	113.19	196.09
12	0.1	8.41	151.11	-	-
	1	8.57[c]	151.17	111.93	197.00[c]

[a]Was made on ^{15}N-enriched compounds. [b]Shift vs. 90% formamide in *d6*-DMSO. [c]Broad peak. [d]Saturated solution.

The same trend in the chemical shifts as in the solid state could be seen in DMSO. Instead, a series of alkyl phenols in both DMSO and chloroform were analyzed to be able to compare the influence of the solvent on the shifts. The results, presented in Table 4.3, showed that the shift differences were much smaller in chloroform than in DMSO, and that the results for phenols in DMSO mainly are attributed to the amount of sterical crowding around the O-H, resulting in lower chemical shifts.

Since the solid-state and the liquid-state data showed the same trend, it is plausible to assume that the results from solid-state NMR also are attributed to the steric possibilities of the hydroxyl group to form strong hydrogen bonds rather than to the electronic effects from the substituents.

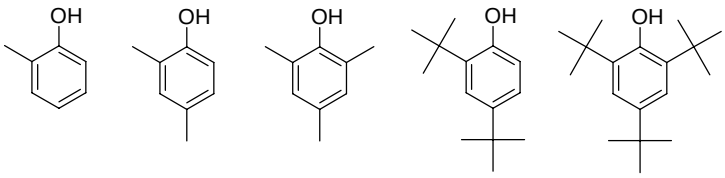

Figure 4.6 Reference phenols for NMR-analysis.

Table 4.3 ^{1}H NMR shifts in ppm in *d6*-DMSO and $CDCl_3$ for the alkyl phenols **14-18**.

Phenol	δ(O-*H*) in *d6*-DMSO	δ(O-*H*) in $CDCl_3$
14	9.18	4.63
15	8.69	4.63
16	7.87	4.43
17	9.06	4.62
18	6.65	5.04

4.3 Phenol, imidazole and water

There is usually a large amount of water in proteins that can be involved structurally in the hydrogen bonded network or play various roles for the function of enzymes. Water molecules are small and mobile and are therefore hard to detect by X-ray diffraction, but they have been revealed in some cases. To study smaller organic molecules containing water, so called organic hydrates, is therefore important for learning more about the role of water molecules in proteins.

The possible hydrogen bonding modes of water are many. The most common situations according to statistical investigations of solved crystal structures, are that the oxygen accepts one or two hydrogen bonds and that the two hydrogen atoms act as donors to two or three hydrogen bond acceptors.[25] A hydrogen bond is postulated when the atoms are within a certain distance from each other.

The X-ray structure of **13** was found to incorporate one molecule of water per molecule of **13**, presumably to avoid having a vacant hydrogen bonding site in the crystal (paper II). Water acts as a donor with its two protons and as an acceptor with the oxygen to one donor, the imidazole (Figure 4.7). The X-ray structure showed that the hydrogen bond distances O…N were slightly longer than the O…N bonds in **10**-**12** (Table 4.4), which could be a result of that the donor ability of water is lower than that of phenol (the pK_a of water is 16 compared to 10 for phenol). The O-H distance in the phenol is the same as in **12**, showing that the imidazole probably has an effect on the phenol via the water molecule.

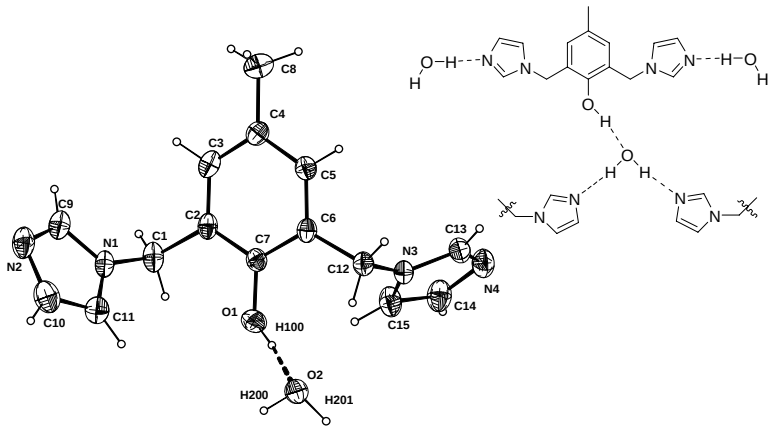

Figure 4.7 ORTEP-picture (30 % probability ellipsoids) of compound **13.**

Table 4.4 Hydrogen bond geometries for **13**.

Hydrogen bond	D-H (Å)	H...A (Å)	D...A (Å)	ΛD-H...A (°)
PhO-H...OH_2	0.94	1.73	2.669	173
HO-H...N	0.94	1.87	2.802	170

An important feature of water molecules are their mobility. A way to probe this is to exchange the proton for deuterium and using ^{2}H NMR. Depending on how mobile they are, the deuterium peak shows different patterns.[104] The ^{2}H NMR spectra of **13** at different temperatures showed that it is almost stationary, even up to temperatures as high as 85°C. This indicates that the hydrogen bonding in the solid is rather strong.

4.4 Conclusions

Examination of the resulting structures of **10-12** suggests that the most important factor determining their three dimensional structure and their hydrogen bond strength is the bulkiness of the *ortho*-alkyl substituent of the phenol. Compound **10**, only having one *ortho*-substituent, can therefore form the best, and a close to optimal, hydrogen bond in the solid state. The ^{1}H NMR solid state measurements were shown to support this satisfactorily. The hydrogen bond in **10** bond probably also closely resembles the one between Tyr_Z and His190 in PSII.

According to ^{2}H NMR, the incorporated water molecule in compound **13** was sitting very tightly, showing that it can form rather strong hydrogen bonds to imidazole and phenol. The water molecule seems to provide good communication between the imidazole and the phenol.

5 Linked phenol-ruthenium compounds

In our studies of photochemically induced electron transfer reactions, Ru(II)trisbipyridine have been used as the photosensitizer. After photo-excitation and oxidative quenching, the generated Ru(III) can act both as an intra- or intermolecular oxidant, as described in chapter 2.5.2. By having the ruthenium chromophor linked to the donor, the electron transfer rate is not limited by diffusion of the two components and faster rates are therefore possible to obtain. For an intramolecular system, the type of linkage is an important factor that influences the electron transfer rate.

The electron transfer kinetics from the Ru(III) to the phenol portion in complex **19** has been studied by time-resolved spectroscopy.[21] We were interested in the effect a modified chain would have on the electron transfer rate and therefore prepared compound **20**. In this chapter, the synthesis of the new compound **20** will be described and its properties discussed.

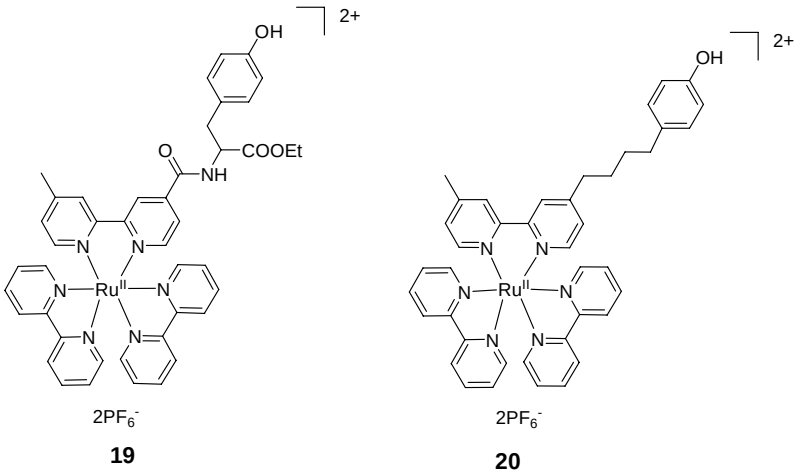

Figure 5.1

5.1 Synthesis

The synthesis of ruthenium complex **20** was started from the commercially available acid **21**. Reduction with lithium aluminium hydride followed by tosylation gave compound **23** that was reacted with 4,4'-dimethyl-2,2´-bipyridine to form compound **25**. After deprotection of the phenol with boron tribromide, the modified bipyridine **26** was coordinated to ruthenium by reacting the ligand with bis-bipyridine ruthenium(II)chloride. After a counterion exchange to PF_6^- the desired ruthenium complex **20** was afforded as a red solid in 53 % isolated yield.

However, the overall yield was rather low, which was mainly due to problems encountered during the purification of compounds **25** and **26**. More synthesis details can be found in appendix A.

Scheme 5.1

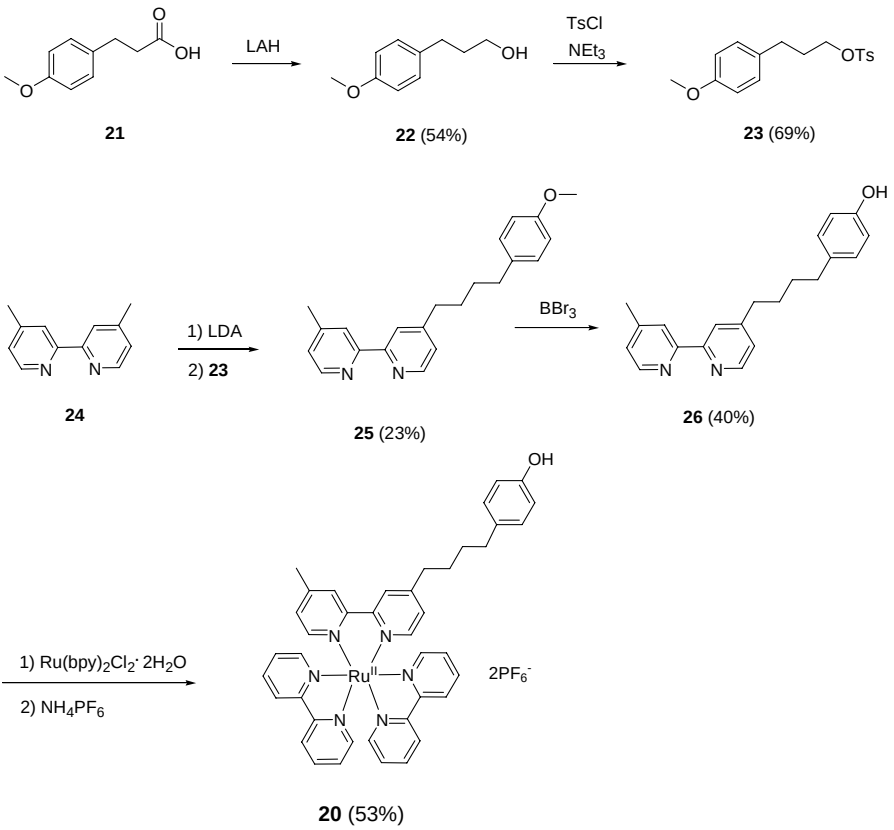

21 **22** (54%) **23** (69%)

24 **25** (23%) **26** (40%)

20 (53%)

5.2 Properties

The absorption spectra of complex **20** in acetonitrile and in aqueous solution at pH = 7.1 are shown in Figure 5.2. Only small differences were found between those two and the one of $[Ru(bpy)_3]^{2+}$. The results indicate that the phenol moiety in **20** is electronically uncoupled to the ruthenium and does not participate in any absorptions of the complex beyond 300 nm.

The fact that the phenyl moiety does not influence the photophysical properties of complex **20** could also be observed in an inspection of the ^{3}MLCT- excited state lifetime. The excited state lifetime of **20** was determined to 0.95 μs in acetonitrile, which is similar to that of $[Ru(bpy)_3]^{2+}$ (0.83 μs under similar condi-

tions). In water at pH 7.1 the lifetime of **20** was 0.49 μs.

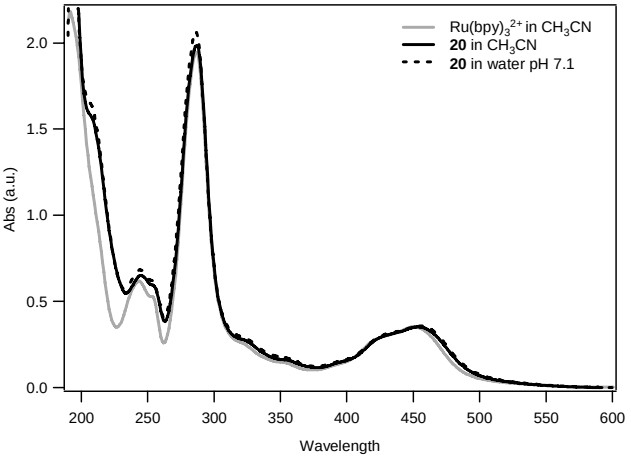

Figure 5.2 Absorption spectra of **20** and $[Ru(bpy)_3]^{2+}$.

Attempts were made to detect intramolecular electron transfer in complex **20** from the phenol to photooxidized Ru(III) in water solution. It was found that the initial amplitude of the Ru(III) signal was rather small and that some of the signal of the $MV^{\bullet+}$ was still present after complete recovery of the Ru(II) signal. This result prompted us to believe that a fast electron transfer could have taken place on a timescale faster than the nanosecond resolution for the experiment. Such a fast electron transfer could well be due to the flexible nature of the alkyl chain, which could fold back the phenol towards the ruthenium and facilitate fast oxidation. Unfortunately, a direct detection of a phenoxyl radical was not possible by using MV^{2+} to generate Ru(III) since the $MV^{\bullet+}$ absorbs in the same region as the phenoxyl radical, slightly above 400 nm.

No electron transfer was observed in dry acetonitrile. After an increasing number of flashes, the absorption spectrum of the complex more and more resembled that of $[Ru(bpy)_3]^{2+}$, indicating that the compound was not stable under the illumination conditions. From an energetic point of view, a proton acceptor has to be present to accomplish electron transfer from the Ru(III) to the phenol, since the redox potential for the phenol would otherwise be too high. No such proton acceptor is provided for **20** in acetonitrile. In water, however, the solvent can provide the necessary proton acceptor and lower the redox potential of the phenol to be in reach for oxidation of Ru(III).

5.3 Conclusions

The alkyl chain is a good linkage in the sense that the electric communication between the redox components is not large. However, the alkyl chain in **20** is probably too flexible to obtain interpretable results from electron transfer experiments from Ru(III) to the phenol. Furthermore, complex **20** was found to be relatively unstable and photodegradation seemed to occur. In summary, a more well defined and robust system is needed.

6 Oxidation of phenols

In this project, collecting information that could be of help for elucidating the mechanism of oxidation and reduction of Tyr_Z, and searching for good models mimicking the function of it, go hand in hand. In this chapter, investigations made on model systems functioning as Tyr_z will be discussed.

Chapter 6.1 deals with oxidation of phenols using different amines as proton acceptors. In chapter 6.2, the results obtained from mechanistic studies on phenols hydrogen bonded to carboxylates as models for carboxylic acid containing amino acids will be presented.

6.1 Hydrogen bonding to amines

Mostly, aliphatic amines have been used to model the hydrogen bond acceptor of Tyr_Z.[23,68,105,106] Those amines, however, are not perfect models for imidazole since the basicity of amines is higher and they lack the aromatic ring system of imidazole.

The main goal with this project was to design and synthesize a system that forms a strong hydrogen bond between imidazole and phenol, and to study its thermodynamic and kinetic properties. In addition, a couple of other amines that contain phenols were studied. The synthesized phenols subjected to investigation are shown in Figure 6.1 and will be discussed separately in different chapters based on their ability to form intra- or intermolecular hydrogen bonds.

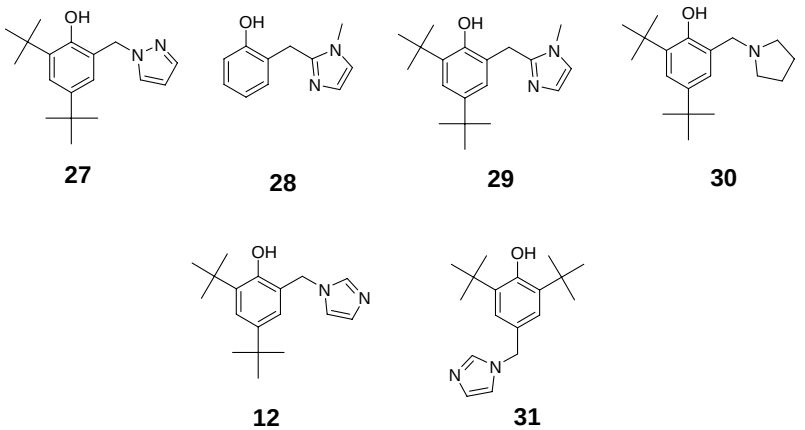

Figure 6.1 Synthesized and studied amine containing phenols.

6.1.1 Synthesis

The main target structure was a phenol that could form an intramolecular hydrogen bond as depicted in Figure 6.2. The performed calculations showed that this particular arrangement of hydrogen bond donor and acceptor would have features close to those of an ideal bond between phenol and imidazole.

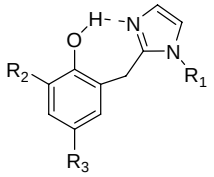

32

Figure 6.2 The target structure.

There are in principal two ways to get to the target compound. Either a modified imidazole moiety can be coupled to a phenol. The other option is to form the imidazole already in place on the phenol. The first step is a ring closure starting from an aldehyde or nitrile to give an imidazoline. It can then be oxidized to the imidazole.

To obtain a structure in which R_1=H in Figure 6.2, a synthesis route was tested in which a protected imidazole (a SEM-group at the 1-position) was lithated in 2-position and reacted with *O*-TBDMS-protected salicylaldehyde.[107] The addition went in rather low yield (46 %) but a larger problem was the residing benzylic hydroxyl group on the carbon-link between the phenol and the imidazole. To get the methylene-linked target structure the hydroxyl group had to be removed. Many procedures were tested but none worked satisfactorily. This route was thus considered too difficult to pursue further.

In parallel, a metal-catalyzed cross-coupling procedure was sought, and this strategy proved to be a better choice. Palladium catalyzed cross-coupling can be used to give rise to a variety of compounds using an organometallic reagent (R-M) and an electrophile, usually a halogenated compound (R'-X) (eq 6.1).

$$\text{R-M} + \text{R'-X} \xrightarrow{[\text{Pd(0)}]} \text{R-R'} + \text{M-X} \qquad (6.1)$$

Test reactions, using easily available 2-lithiated imidazole with benzyl bromide with and without the presence of $PdCl_2(PPh_3)_2$, afforded no desired product, possibly due to the acidic benzylic protons that could be abstracted by the basic lithium reagent. Therefore less basic transmetalating agents were investigated. Zinc compounds were chosen, which have been widely used in Negishi couplings and are known to be mild transmetallating agents in Pd-couplings.[108]

The metal-reagent could either contain the phenol or the imidazole moiety. Benzylic metal reagents can be synthesized but the reaction is not trivial since the formed reagent can react with the remaining benzylic halide to give symmetrical substituted 1,2-diphenylethanes. On the other hand, the use of benzylic

halides in Pd-catalyzed cross-coupling reactions can also be problematic due to competing homo-coupling and problems in the oxidative addition step.

A suitable procedure was found for the synthesis of benzylic zinc-reagent **34** which could be used in a Pd-catalyzed cross-coupling with 2-iodo-1-methylimidazole to yield 68% of **35** (Scheme 6.1). The choice of using 1-methylated imidazole was made since methyl is a small protecting group that can be kept in the final product (R_1=CH_3 in Figure 6.2) without disturbing the formation of an intramolecular hydrogen bond significantly.

Scheme 6.1

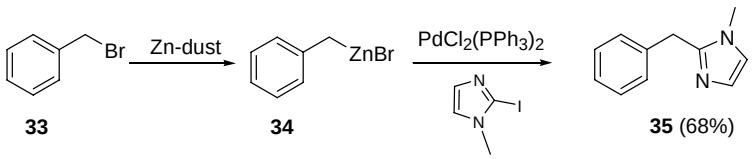

33 **34** **35** (68%)

Synthesis of zincreagents **40** was accomplished from the methoxy substituted benzyl bromides **39** synthesized according to standard procedures (Scheme 6.2). The Pd-coupling protocol used for **35** could be employed for couplings between zincreagents **40** and 2-iodo-1-methylimidazole (**42a**) to give 62% of **43a** and 89% of **43b**, respectively**.** $Pd(OAc)_2$ and tri(*o*-tolyl)phosphine were used instead of $PdCl_2(PPh_3)_2$ since this combination gave a slightly cleaner crude product mixture according to ^{1}H NMR. Demethylation of the hydroxyl group could be accomplished by using boron tribromide to give the final products **28** and **29**.

Scheme 6.2

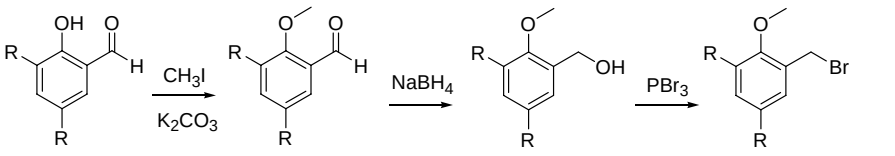

36 R= *t*-Bu **37** R=*t*-Bu (47%) **38a** R=H **38b** R= *t*-Bu (94%) **39a** R= H (81%) **39b** R= *t*-Bu (88%)

Scheme 6.3

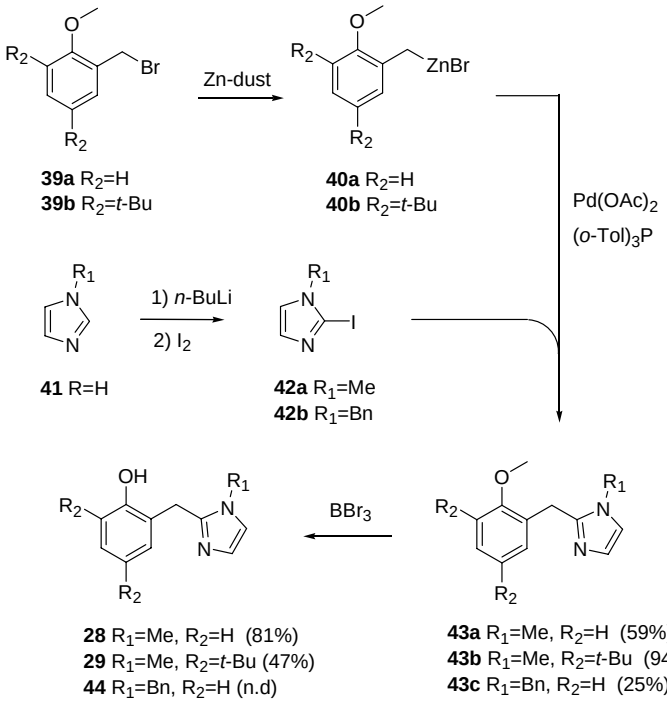

39a R_2=H
39b R_2=*t*-Bu

40a R_2=H
40b R_2=*t*-Bu

41 R=H

42a R_1=Me
42b R_1=Bn

28 R_1=Me, R_2=H (81%)
29 R_1=Me, R_2=*t*-Bu (47%)
44 R_1=Bn, R_2=H (n.d)

43a R_1=Me, R_2=H (59%)
43b R_1=Me, R_2=*t*-Bu (94%)
43c R_1=Bn, R_2=H (25%)

In an attempt to obtain an imidazole with a readily removable 1-N substituent using this route, 2-iodo-substituted *N*-benzyl-imidazole **42b** was synthesized and tested in the Pd-coupling together with **40a**. However, the maximum yield of **43c** turned out to be only 25% indicating that the coupling reaction seems to be sensitive to sterical hindrance on the imidazole part.

The reaction to get to **10-13** in chapter 4.1 worked equally well for trisubstituted benzylalcohols **45** and **46**, and by using pyrazole (Scheme 6.4) and imidazole (Scheme 6.5) as nucleophiles compounds **27** and **31** could be obtained.

Scheme 6.4

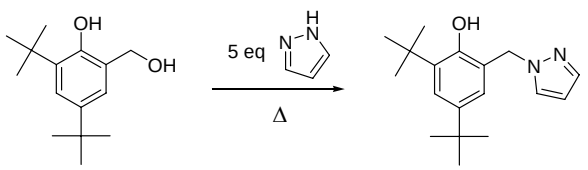

45

27 (68%)

Scheme 6.5

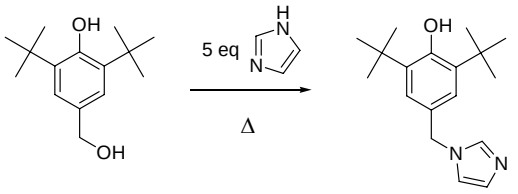

46 **31** (87%)

Compound **30** was synthesized in a one step Mannich reaction from 2,4-di-*t*-butylphenol (**47**), pyrrolidine and para-formaldehyde.[68]

Scheme 6.6

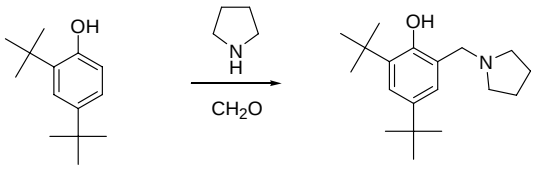

47 **30** (80%)

6.1.2 Intramolecular systems

Considering the basicity of their amines, **30** has the most favorable conditions to form a strong hydrogen bond to phenol.

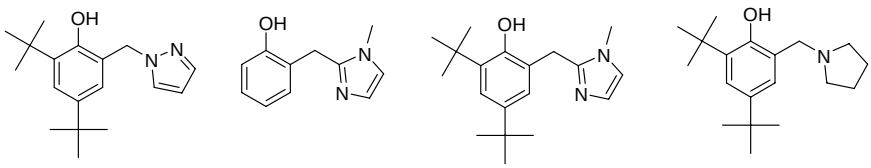

27 **28** **29** **30**

Figure 6.3 The studied phenols with possibility of forming intramolecular hydrogen bonds.

To analyze this experimentally for compounds **27-30,** the chemical shifts for their hydroxyl protons were determined in four different solvents with ^{1}H NMR (Table 6.1). The δ for all compounds in all solvents were high compared to non-hydrogen bonded phenols (for examples, see chapter 4). The values were also rather independent of the solvent (compare with NMR-results in chapter 6.1.3), pointing toward that the formed hydrogen bonds were intramolecular. Compound **30** had the highest chemical shifts (around 11-11.5 ppm), followed by 2**8** and **29** (between 10 and 11 ppm) and **27** (around 10 ppm). The trend is following the ones for the intermolecular models studied with calculations, which are in-

cluded in Table 6.1. Calculations were only conducted on non-substituted phenol models, therefore the values are the same for **28** and **29** in the table.

Table 6.1 Data for the hydrogen bonds of **27-30**.

	^{1}H NMR δ of O-*H* 0.1 M solution (ppm)				I_{HB} from calculations (kcal/mol)	
	Benzene	**$CDCl_3$**	**Acetonitrile[a]**	**DMSO**	**Intra-HB[d]**	**Inter-HB[e]**
27	10.7	10.1	10.1	9.6	6.0	9.1
28	-[c]	~10[b]	11.2	~10[e]	9.1	9.7
29	11.3	10.7	11.0	11.0	9.1	9.7
30	11.4	11.5	10.9	11.5	7.8	10.5

[a]Concentration 0.017 M. [b]Very broad peak. [c]Not soluble. [d]The unsubstituted intramolecularly hydrogen bonded version. [e]The corresponding intermolecular systems with optimal hydrogen bonds.

All compounds showed oxidation peaks at lower potentials in acetonitrile than their corresponding reference amines in CV, as seen in Table 6.2. The peaks were assigned to oxidation of the hydrogen bonded phenols, *i.e.* upon oxidation the proton is abstracted by the amine (as already proposed for **30**). The potentials for oxidation of alkyl substituted phenols are around 1 V vs. ferrocene, Fc, depending on the exact substituents of the phenol.

Table 6.2 Data for oxidations of **27-30** from CV, kinetic experiments using Ru(III) and calculated ionization potentials.

	E_{pa} (V vs. $Fc^{+/0}$)[d]	E_{pa} of ref. amine[c] (V vs. $Fc^{+/0}$)[d]	k_{ET} ($M^{-1}s^{-1}$)	IP from calculations Intra-HB[a] (kcal/mol)	Inter-HB[b] (kcal/mol)
27	0.74	1.59	$1.2 \cdot 10^6$	167.8	162.3
28	0.42	1.20	$8.3 \cdot 10^7$	157.9	155.7
29	0.36	1.20	$1.4 \cdot 10^8$	157.9	155.7
30	0.25	0.39	$1.6 \cdot 10^8$	158.7	151.4

[a]The unsubstituted intramolecularly hydrogen bonded version. [b]The corresponding intermolecular system with an optimal hydrogen bond. [c]The corresponding 1-methylated amine. [d]The anodic peak potential for oxidation in acetonitrile.

The rate with which the phenols could be oxidized with Ru(III) was correlating well with the potentials required for oxidation. Spectroelectrochemisty, a method in which a spectrum of the solution is recorded keeping the solution at a fixed potential, showed typical phenoxyl radical spectra with two sharp peaks around 400 nm and a broader one at longer wavelength for **27** and **30**.

The oxidations of **27**, **29** and **30** were partly reversible in CV, showing that

the formed radicals were fairly stable. Phenol **28** was not expected to show a reversible oxidation due to the lack of phenol substituents stabilizing the formed radical. The substituted phenol **29** was slightly easier to oxidize than **28** due to the more electron rich ring.

The oxidation of phenol **29** showed the same behavior upon oxidation as the others did; its oxidation definitely was due to the hydrogen bond and generated a phenoxyl radical, though a different and more complicated behavior was seen on a longer time scale after the generation of the radical. With spectroelectrochemistry, the resulting spectrum changed from phenoxyl radical like to a spectrum having the features shown in Figure 6.4. A similar behavior was seen in chemical oxidation experiments using $Cu(ClO_4)_2$ in acetonitrile. An excess of Cu-salt gave a phenoxyl radical like spectrum. On the other hand, using an excess of the phenol directly gave the strongly absorbing species seen as a secondary product in spectroelectrochemistry. Since more secondary species are formed upon use of an excess of phenol, it is reasonable to assume that the phenoxyl radicals are reacting with unoxidized phenols. What the secondary product might be is so far unknown.

Since the secondary products are formed even at such a low potential as used in spectroelectrochemistry, this structural arrangement might be less suited for participating in electron transfer systems. Nevertheless, the oxidation showed rather high reversibility indicating that if the oxidations and reductions are fast enough, the phenol could be appropriate anyway.

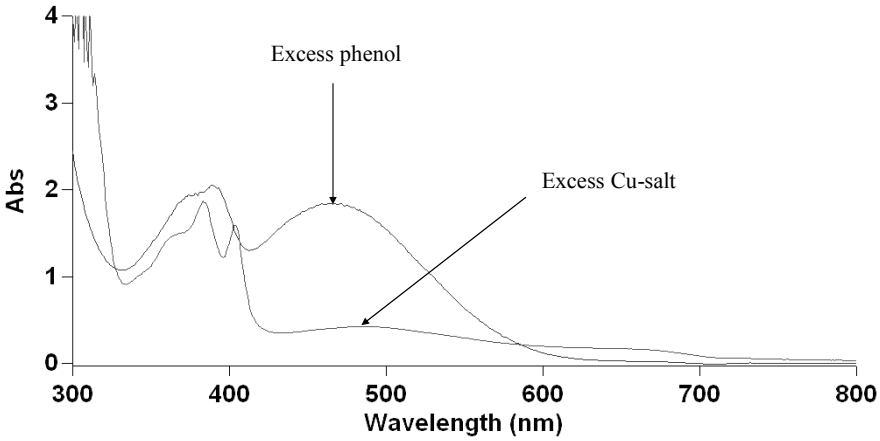

Figure 6.4 UV-Vis spectrum of the products from oxidation of **29** with $Cu(ClO_4)_2$ in acetonitrile using an excess of phenol or an excess of the copper salt.

In a system for multi-step electron transfer, the stability of the radicals do not have to be extremely high, such as the ones presented here with *tert*-butyl groups, but for studying the properties as made in this study the stability is a great advantage. A phenoxyl radical would only exist as a transient radical if generated in a system in which the phenol is acting as an intermediate redox

component. If the electron transfer events are fast, the radical would not have to have to be a stable one (with a half live > 10^{-3} s) but a shorter life time might be sufficient.

A natural step when finding a good electron transfer mediator would be to couple it to the photosensitizer. Unfortunately, how fast intramolecular electron transfer reactions can be studied with this type of photochemical initiation is limited by the reaction that creates Ru(III), *i.e.* the intermolecular electron transfer from *Ru(II) to MV^{2+}. The rate of electron transfer from a very fast intramolecular electron donor would therefore not be possible to resolve. This means that there is no use of coupling a too fast electron donor to $[Ru(bpy)_3]^{2+}$ to form a dyad. To be able to investigate such a system an intramoleular electron acceptor instead of MV^{2+} in solution would be required.

6.1.3 Formation of intermolecular complexes

Another way to obtain hydrogen bonds between imidazole and phenols is to let them form intermolecular hydrogen bonds in solution. Figure 6.5 shows the studied systems that could form intermolecular hydrogen bonds. The degree of association highly depends on the solvent properties, the character and concentration of the donors and acceptors and the conditions in general in the solution.

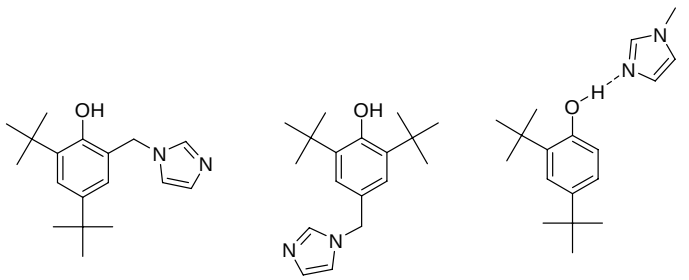

12 **31** **48**

Figure 6.5

It was found that compound **12** formed stable phenoxyl radicals with oxidation using $Cu(ClO_4)_2$ in acetonitrile, generating the same radical UV-Vis spectrum as the one for **30**, even though it was lacking a strong intramolecular hydrogen bond. DFT-calculations on the conformation of the molecule that could have an intramolecular hydrogen bond showed not much extra stabilization for that conformation (Figure 6.6). ^{1}H NMR showed that in acetonitrile **12** associated only to a small extent compared to the compounds discussed in the previous chapter (Table 6.3). The chemicals shift were similar to 2,4-di-*tert*-butylphenol mixed with 1-methylimidazole (**48**).

Table 6.3 ^{1}H NMR δ of O-*H*, 0.1 M solution for the studied intermolecular systems and a reference phenol.

	Benzene (ppm)	**$CDCl_3$ (ppm)**	**Acetonitrile [a] (ppm)**	**DMSO (ppm)**
12	10.6	6.4	6.5	5.7
31	5.7	5.3	5.6	7.7
48[b]	11.0	5.8	8.1	9.1
47	3.8	4.6	6.7	9.0

[a]0.017 M. [b]A 1:1 mixture.

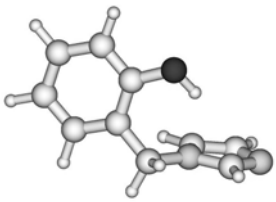

Figure 6.6 A conformation of an unsubstituted version of **12** that could have an intramolecular hydrogen bond.

A complexation constant for the equilibrium between hydrogen bonded and non-hydrogen bonded 2,4-di-*tert*-butylphenol and 1-methylimidazole (system **48**) could be found by analyzing the ^{1}H chemical O-*H* shifts of different mixtures of the donor and the acceptor using NMR. The complexation constant was found to be only 3.6 M^{-1}, implying that in a 1:1 mixture with a concentration of 0.1 M, only one fifth of the molecules are hydrogen bonded in average.

Also the rate constant for electron transfer from 2,4-di-*tert*-butylphenol to Ru(III) was determined as a function of the concentration of 1-methylimidazole (the system **48**). A dependence of the rate constant for electron transfer was found that was almost identical to the one obtained from the concentration study for **48** with NMR. It gave a complexation constant of 3.5 M^{-1}, as compared to 3.6 obtained with NMR. This means that the measured electron transfer rates with Ru(III), k_{obs} were simply reflecting the amount of hydrogen bonded species in solution (equation 6.2). The fractions of hydrogen bonded resp. non-hydrogen bonded species are x_{HB} and (1- x_{HB}) For this system the rate constant for electron transfer from the hydrogen bonded complex is much larger than the one for the non-hydrogen bonded phenol, $k_{HB} >> k_{PhOH}$, because the solvent, acetonitrile, can not accept any protons in contrast to for example water.

$$k_{obs} = x_{HB} \cdot k_{HB} + (1 - x_{HB}) \cdot k_{PhOH} \qquad (6.2)$$

The rate constant for electron transfer from the hydrogen bonded species k_{HB} is the value that the constant approaches when the Me-Im concentration goes to-

wards infinity. This value for **48,** $3.4 \cdot 10^8\ M^{-1}s^{-1}$, is in the same range as the rate constant obtained for the phenol intramolecularly hydrogen bonded to imidazole **29**, $1.4 \cdot 10^8\ M^{-1}s^{-1}$.

Table 6.4 Data for oxidations of **12** and **31** from CV and kinetic experiments using Ru(III).

	E_{pa} (V vs. $Fc^{+/0}$)	E_{pa} of ref. amine[a] (V vs. $Fc^{+/0}$)	k_{ET} ($M^{-1}s^{-1}$)
12	0.29	1.2	$2.4 \cdot 10^6$
31	0.41	1.2	-[b]

[a]1-Methylimidazole. [b]Not observed.

Oxidation with CV, in contrast to oxidation with Ru(III), showed clearly the effect of hydrogen bonds of **12** in solution. This is due to a shifting of the hydrogen bond equilibrium during the experiment, as shown by a concentration study also with DPV for 2,4-di-*tert*-butylphenol and 1-methylimidazole. An oxidation wave for hydrogen bonded phenol immediately appeared at the value for hydrogen bonded phenol, even though the imidazole concentration was only 1/7 of the phenol concentration. A similar behavior was seen by Linschitz *et al.* for oxidation of phenols hydrogen bonded to different amines.[64] For **12** this effect of the shift of the equilibrium can be seen as a larger peak-split between the anodic and cathodic peaks in CV as compared to **30** for example.

The stability of the phenoxyl radical of **12** is quite remarkable and is the only one of the phenol-amine systems studied here in which both spectroelectrochemistry and chemical oxidation using $Cu(ClO_4)_2$ show a clear phenoxyl radical spectrum that is stable for a longer period of time. In compound **31,** the sterical hindrance exerted by the two *tert*-butyl groups prevents a good hydrogen bond interaction with the imidazole in the *para*-position of other molecules. The compound is still rather easily oxidizable (0.41 V of the anodic peak vs. $Fc^{+/0}$), but there is not much reversibility of the oxidation, showing that good hydrogen bonding is required for reversibility, but not for oxidation on the time scale of the CV experiments. This is in line with what has been concluded by others: that the stability of the formed radical is affected by hydrogen bonding.[109,68]

6.1.4 Conclusions

A close structural and functional model for the Tyr_Z-His190 parts of PSII, **29**, has been synthesized and studied. The bimolecular electron transfer reaction from Ru(III) is as fast as from phenol-amine hydrogen bonded system.

The hydrogen bond equilibrium can shift on the time-scale of the experiment, in contrast to in kinetic experiments using Ru(III). There only the hydrogen

bonded fraction of the phenols can be oxidized. A good hydrogen bond interaction to the phenol is required to obtain a close to reversible trace of it in CV.

6.2 Hydrogen bonding to carboxylates

In the proximity of Tyr_Z in PSII there is also a carboxylate (Glu189) that could take part in the redox and proton transfer events at the site. Carboxylates have pK_a-values around 4 and could act as proton acceptors for phenoxyl radical cations.

The oxidation-kinetics of **49**-**50** was studied with the same type of flash photolysis experiments using Ru(III) described earlier. Also pulse radiolysis, which is another method with which radical-reactions can be studied, was used to oxidize the compounds. The oxidant used is a stronger oxidant than Ru(III): $Br_2^{\bullet-}$ (1.6 V vs. NHE). Pulse radiolysis was also used to study the redox properties of the phenols.

Since the experiments were conducted in water solution, *tert*-butyl substituted phenols, as in the previous chapter, were not used.

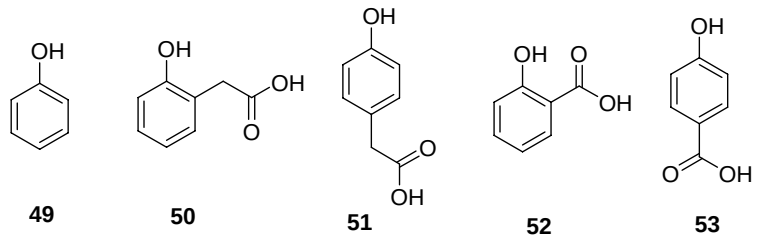

Figure 6.7 The investigated phenols.

6.2.1 Hydrogen bonding and redox properties

Quantum chemical calculations on the compounds **50**-**53**, similar to the ones performed for the amines in chapter 6.1, were attempted but failed. The calculations seemed to suffer heavily from the absence of a proper surrounding in the models, i.e. explicit interactions from solvent molecules. Modeling the solvent (water) with an electric field was tested but it did not seem to be sufficient.

^{1}H NMR could not be used for studying the hydrogen bonds. The only proper solvent for analysis that would definitely prevent the aggregation that is known to occur for these type of compounds, would be D_2O.[47] Due to the fast H to D exchange, the peaks for the O-H would not be possible to observe in water.

An indication of hydrogen bonding could be seen in the pK_a-values of the compounds (Table 6.5). Carboxylate substitution of a phenol should give a slightly lower pK_a value than of phenol (~10). That is seen for **53** with a pK_a value of 9.1. Compound **52** on the other hand has a pK_a-value of 13.5. This is an

indication on intramolecular hydrogen bonding. The pK_a for compound **51** shows that the methylene carboxylate substituent does not alter the phenol pK_a much (pK_a of **51** is only slightly higher than for the phenol, **49**). Compound **50** has a somewhat higher value than **51**, which could be a result of a weak hydrogen bond interaction.

The reduction potentials of the compounds can be seen in Table 6.6. In the PCET-region (the pH-interval where proton coupled electron transfer can occur) the proton would be transferred from the phenol upon oxidation, either to water directly or to water via the internal carboxylate (in the phenols that are *ortho*-substituted). As long as the pH-value of the solution is kept above the pK_a value of the carboxylate, the proton does not stay on the carboxylic acid if it is abstracted by it. Provided that all phenols would only be involved in interactions with the surrounding water, the start and end states in the oxidation processes for them would be the same. Hydrogen bonding to either the start or end state could have an impact of the redox potential of the phenol, as discussed previously in the thesis. This implies that the redox potentials of the compounds could say something about the hydrogen bond situation the compounds.

Compound **52** is more difficult to oxidize than **53** at pH 7 (the $E^{0'}$ in Table 6.6). This could be an effect of hydrogen bonding according as explained above. The strong hydrogen bonding in the salicylate **52** has a quite stabilized starting state for oxidation, which increases the energy difference between its reduced and oxidized forms, resulting in a higher reduction potential. In fact, the difference in reduction potential between **52** and **53**, about 0.1 V, gives an approximation of the hydrogen bond strength. Compounds **50** and **51** on the other hand have the same potentials, indicating that no strong hydrogen bond are involved in deciding the potentials suggesting that the intramolecular hydrogen bond in **50** is weak.

Table 6.5 pK_a-values for the investigated phenols.

Phenol	pK_a (PhOH)	pK_a (COOH)
49	10.0[b]	-
50	10.9[a]	4.3[a]
51	10.3[a]	4.3[a]
52	13.5[b]	3.1[b]
53	9.3[b]	4.5[b]

[a]Determined by pH-titration.[b]Reference [110].

Table 6.6 Reduction potentials vs. NHE for the investigated phenols.

Phenol	E^0 ($PhOH^{\bullet+}$/PhOH) (V)[b]	$E^{0'}$ ($PhO^{\bullet+}$/PhOH) vid pH = 7 (V)[b]	E^0 ($PhO^{\bullet}/PhO^-$)[a] (V)
49	1.49	0.96	0.78
50	1.42	0.94	0.71
51	1.46	0.94	0.75
52	1.48	1.15	0.77
53	1.49	0.96	0.78

[a]Determined by pulse radiolysis. [d]Calculated from the E^0(PhenO•/$PhenO^-$) value (see paper V).

6.2.2 Mechanism of electron transfer

The goal of the kinetic measurements on **49-53** was to study what PCET-mechanisms the oxidation of the phenols in Figure 6.7 go via. The rate of electron transfer to photogenerated Ru(III) (by the flash quench method) from phenol **49** was determined in water solution at different pH. The results can be seen in Figure 6.8 (the dots). The observed k_{ET} values are a sum of the contributions from the two different species in solution, the phenols and the phenolates. However, the simple equations 6.3 and 6.4 describing the titration of the phenol, resulted in a curve which did not follow the observed rate constants well (the broken line in Figure 6.8). The α is the fraction protonated phenols. The problem with this treatment was that the pH-dependence of the CEP-mechanism, taking place in the PCET-region (the region where most phenols are protonated) was not taken into account.

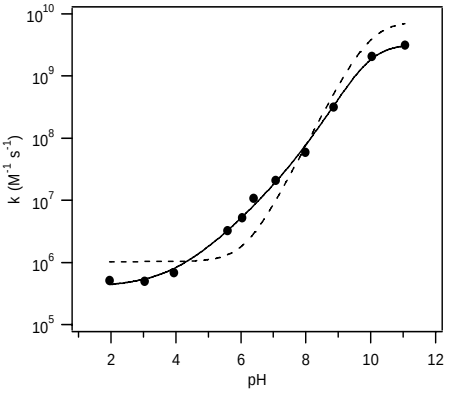

Figure 6.8 The dependence of the rate of electron transfer from phenol to Ru(III) on the pH. The line is a fit to equation 6.5.

$$k = \alpha\, k_{PhOH} + (1-\alpha)\, k_{PhO^-} \qquad (6.3)$$

$$\alpha = (1 + 10^{pH-pKa})^{-1} \qquad (6.4)$$

By introducing a pH-dependent rate constant $k_{CEP}=k_{CEP}^{0}10^{\gamma pH}$, a good fit to the experimental data was obtained (the line in Figure 6.8). This expression was derived from the semi-classical Marcus-equation (see paper V). The k_{CEP}^{0} (the rate for CEP at pH=0) and γ are constants. A correction for ETPT (k_{ETPT}) was also added to account for the ETPT taking place at low pH. Thereby the rate constant for the phenol, k_{PhOH}, was consisting of two separate factors (equation 6.5). At pH-values below 4 the results show that the rate constant of electron transfer from the phenol becomes independent of pH and the ETPT becomes the dominating mechanism. Above pH 4 the CEP-mechanism dominates.

$$k = \alpha\, (k_{ETPT} + k_{CEP}^{0}10^{\gamma pH}) + (1-\alpha)\, k_{PhO^-} \qquad (6.5)$$

For the phenols with *para*-substitution, **51** and **53**, lacking the possibility of forming intramolecular hydrogen bonds, the rates of electron transfer were rather similar to the ones for the simple phenol. Equation 6.5 had only to be adjusted for the two different forms of the carboxylic acids: $f_{(a)}$ and $f_{(b)}$ are the fraction phenols with protonated resp. deprotonated acids. The new equation 6.6 was obtained.

$$k = \alpha\, (k_{ETPT} + (f_{(a)}\, k_{CEP(a)}^{0} + f_{(b)}\, k_{CEP(b)}^{0})10^{\gamma pH}) + (1-\alpha)\, k_{PhO^-} \qquad (6.6)$$

For the phenols having a possibility of forming intramolecular hydrogen bonds, **50** and **52**, the obtained k_{ET}-values seemed to have a pH-region above the carboxylic acid pK_a, where k was independent of pH, in contrast to **51** and **53** (Figure 6.9). This could be due to an intramolecular proton transfer from the phenol to the carboxylate upon oxidation of the phenol, which would be independent of pH since the carboxylate will practically have the same effect at all pH values as long as it is deprotonated. In equation 6.7 this was taken into account by insertion of the term $f_{HB}k_{HB}$.

The resulting equation 6.7 is then divided into two parts: one for the protonated phenols, preceeded with α, and one for the phenolates, proceeded by $(1-\alpha)$. In turn, the first term consists of two parts: one for the molecules that have protonated carboxylates (the $f_{(a)}$–term) and one that takes care of the phenols with deprotonated carboxylates, $f_{(b)}$. Even if the carboxylate is deprotonated, it is not certain that there is intramolecular hydrogen bonding in all molecules, therefore the $f_{(b)}$-fraction also needs to be divided into two parts: one for the non-hydrogen bonded fraction f_{NHB} and one for the hydrogen bonded molecules f_{HB}, each having their own respective rate constants for electron transfer. The term for ETPT was found to be negligible.

$$k = \alpha(\, f_{(a)}(k^{0}_{CEP(a)}10^{\gamma pH}) + f_{(b)}(f_{NHB}k^{0}_{CEP(b)}10^{\gamma pH} + f_{HB}k_{HB})) + (1-\alpha)k_{PhO^-} \qquad (6.7)$$

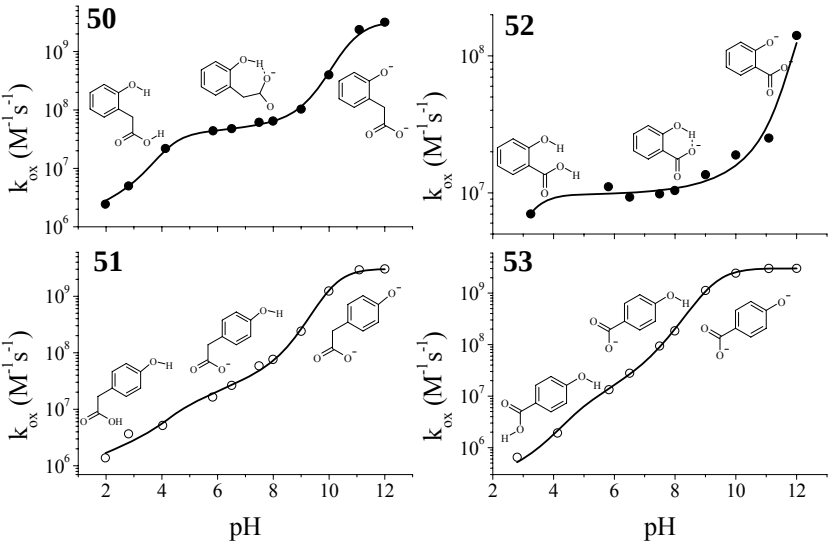

Figure 6.9 The dependence of the rate constants for electron transfer for **50**-**53** (dots and circles). The lines are fits to the derived equations (see above).

Oxidation of compounds **50**-**53** was also accomplished using pulse radiolysis. The use of a stronger oxidant favors ETPT over CEP, and the electron transfer rates could indeed be assigned to follow the ETPT-mechanism in the pulse radiolysis experiments in the PCET-region at pH 5-8 (see paper V). A similar reasoning could rule out ETPT for the oxidation experiments with Ru(III), and thereby also from being responsible for the pH-independence seen in the PCET-region for **50** and **52**.

The pH-independence seen for **50** and **52** could also not be the result of PTET, since to account for the high electron transfer rates observed, the oxidation of the phenolates would have to be many times the diffusion controlled rate. Hence the PTET-mechanism could also be ruled out.

Left is then only the CEP mechanism for oxidation of **50** and **52** in the pH-independent region, and it has to take place with proton transfer internally to the carboxylate, otherwise a pH-dependence would be seen.

The rate of oxidation of **50** and **51** as well as of **52** and **53** were very similar in the PCET-region, even though their driving forces for electron transfer are different; it is more favorable to release a proton to a pH 7-solution than to a base with a pK_a-values of 3-4, as for the carboxylate. We suggest that the rate constants in the hydrogen bonded systems are high, despite the low driving force, due to a decrease in reorganization energy for the oxidation process due to a smaller distance for the transfer of the proton.

6.2.3 Conclusions

In the PCET-region of the phenols, they are oxidized via a concerted electron and proton transfer mechanism, either to the bulk (in the case of non-hydrogen bonded phenols) or to the internal carboxylate (for the intermolecularly hydrogen bonded phenols). The rates of electron transfer are increased for the internally hydrogen bonded models, which could be due to a decrease in reorganization energy.

7 Concluding remarks

In this thesis a model phenol with a hydrogen bond interaction, closely resembling the one presumed for Tyr_Z-His190 in PSII, is presented. The investigations of its properties show that the imidazole has a significant impact on the redox properties of the phenol; it is almost as big as the one of the more basic and more studied proton acceptor, tertiary amine. It was also shown that the quality of the hydrogen bond interaction between imidazole and phenol is not particularly sensitive to the exact arrangement of the hydrogen bond donor and acceptor. This might have implications for the function of the two moieties in enzymes.

The high reduction potential of imidazole makes it a good choice as a proton acceptor for a phenol in a system for multistep electron transfer. A drawback of imidazole-compounds, however, is their sometimes difficult synthesis and purification.

Furthermore, the mechanism by which proton coupled electron transfer takes place was studied in the case of phenols hydrogen bonded to carboxylates. It was shown that the dominating mechanim in the PCET-region was the concerted proton and electron transfer mechanism, CEP. Much more remains to be done in this area of kinetic effects of hydrogen bond acceptors to phenol, and to elucidate exactly what the effect is due to.

A big challenge for the future is how to arrange different redox components spatially to obtain simple systems with the desired properties that also do not require too extensive syntheses. This thesis presents some research directions towards a solution for this problem.

Appendix A) Comment on my contribution to this work

I have been performing all synthesis in the papers and all calculations. I have been making the NMR analysis in the liquid state and the chemical oxidation experiments that have been followed with UV-Vis. I have also been the main writer of papers I-IV. I have made some background studies and taken part in the discussions for paper V.

Appendix B) Synthesis of compound 20.

All reactions were performed under inert gas.

3-(4-Methoxy-phenyl)-propan-1-ol (22). 3-4(methoxyphenyl)propionic acid (**21**) (0.5 g; 2.8 mmol) was added to a dried flask together with dry ether (5 ml). 1 M LAH in THF (6.2 ml; 6.2 mmol) was added dropwise over 15 min and after an hour the solution was heated to reflux for 4 h. After cooling to rt, ethylacetate was added followed by water. The organic layer was washed with 2 x 0.1 M NaOH(aq) and dried with Na_2SO_4. Evaporation of the solvent afforded 0.4 g of a pale yellow oil (88%) that could be directly taken to the next step. ^{1}H NMR ($CDCl_3$, 300 MHz) δ = 7.12 (d, 2H, *J*=8.9 Hz), 6.83 (d, 2H, *J*=8.9 Hz), 3.67 (t, 2H, *J*=6.0 Hz), 2.66 (t, 2H, *J*=7.6 Hz), 1.86 (tt, 2H, *J*=6, 7.6 Hz) 1.45 (s, 1H).

Toluene-4-sulfonic acid 3-(4-methoxy-phenyl)-propyl ester (23). The alcohol **22** (0.91 g; 5.5 mmol) and triethylamine (1.5 ml; 10.8 mmol) was dissolved in dry dichloromethane (7 ml). During 2 h, freshly purified *p*-toluenesulphonylchloride (1.36 g; 7.1 mmol) dissolved in dichloromethane (8 ml) was added once every 10th minute to the reaction mixture kept at 0° C. The mixture was allowed to heat up to rt and was stirred over night. The solution was then poured in to water. The layers were separated and the organic layer was washed with 2 x 4 M HCl, 1 x Na_2CO_3 (satd) and 1 x water and dried with Na_2SO_4. The crude product obtained after evaporation of the solvent was purified with column chromatography using as gradient from 1:9 ethylacetate/pentane to 1:1. This gave 1.04 g (59%) of **23** as colorless crystals. ^{1}H NMR ($CDCl_3$, 400 MHz) δ = 7.79 (d, 2H, J=8.0 Hz), 7.34 (d, 2H, *J*=8.0 Hz), 6.98 (d, 2H, *J*=8.4 Hz), 6.77 (d, 2H, *J*=8.4 Hz), 4.02 (t, 2H, *J*=6.2 Hz), 3.78 (s, 3H), 2.59 (d, 2H, *J*=7.2 Hz), 2.46 (s, 3H), 1.92 (app quint, 2H, *J*=7.2 Hz).

4'-[4-(4-Methoxy-phenyl)-butyl]-4-methyl-[2,2']bipyridine (25). Freshly distilled diisopropylamine (0.43 ml; 3.08 mmol) was dissolved in dry THF and cooled to -60° C. *n*-Butyllithium, 1.6 M in hexanes, (1.93 ml; 3.08 mmol) was added dropwise and the mixture was stirred for 1 h. A solution of 4,4'-Dimethyl-[2,2']bipyridine (**24)** (0.49 g; 2.68 mmol) in THF (11 ml) was added over 20 min. After additionally 45 min the tosylate **23** dissolved in THF (9 ml) was added dropwise and the mixture was heated at reflux over night. Water was added and the layers were separated. Two times extraction with dichloromethane was made followed by evaporation of the solvent. Column chromatography

using ethylacetate/pentane 1:1 with a couple of percent of triethylamine followed by recrystallization from methanol afforded 0.25 g (23%) of round-shaped colorless crystals. ^{1}H NMR ($CDCl_3$, 300 MHz) δ = 8.55 (d, 2H, *J*=5 Hz), 8.23 (s, 2H), 7.14-7.06 (m, 2H), 6.81 (d, 2H, *J*=8.7 Hz), 3.78 (s, 3H), 2.72 (t, 2H, *J*=6.9 Hz), 2.59 (t, 2H, *J*=7.8 Hz), 2.44 (s, 3H), 1.74-1.65 (m, 4H).

4-[4-(4'-Methyl-[2,2']bipyridinyl-4-yl)-butyl]-phenol (26). Borontribromide (0.12 ml; 1.2 mmol) and **25** (0.10 g; 0.31 mmol) was dissolved in dichloromethane (5 ml). For 1 ½ h the solution was heated at reflux. After cooling to rt, water was added slowly followed by chloroform. NaOH (aq) was used to adjust the pH to ~10 and three more extractions with chloroform of the water layer were made. The combined organic layers were evaporated and the residue was purified with column chromatography using an eluent of ethylacetate/pentane 1:1 together with a couple of percent of triethylamine. This afforded 0.021 g (21%) of **26** as colorless crystals. ^{1}H NMR ($CDCl_3$, 400 MHz) δ = 8.54 (dm, 2H, *J*=4 Hz), 8.21 (d, 2H, *J*=10.4 Hz), 7,11 (dm, 2H, *J*=10.4 Hz), 7.00 (d, 2H, *J*= 7.6 Hz), 6.73 (d, 2H, *J*=7.6 Hz) 2.67 (t, 2H, *J*=7.6 Hz), 2.54 (t, 2H, *J*=7.2 Hz) 1.71-1.65 (m, 4H).

$[Ru(bpy)_2(4)][PF_6]_2$ (20). Compound **26** (0.026 g; 0.082 mmol) was dissolved in degassed ethanol (4 ml). $Ru(bpy)_2Cl_2 \cdot 2H_2O$ (0.04 g; 0.077 mol) was added and the solution was heated to reflux for 3 h. After cooling to rt water was added (8 ml). The water layer was washed with chloroform four times and NH_4PF_6 (0.033 g; 0.2 mmol) was added. The ruthenium complex was extracted out with 3 x dichloromethane and evaporated. The crude product was put on a column using acetonitrile/water/KNO_3 20:3:1 as an eluent. The fractions containing the products were combined and NH_4PF_6 (0.041 g; 0.25 mmol) was added and the product was extracted with 2 x dichloromethane and the solvent evaporated. This gave 0.042 g (53%) of **20** as a red solid. ^{1}H NMR (*d6*-acetone, 300 MHz) δ = 8.82 (d, 4H, J=8.1 Hz), 8.71 (s, 2H), 8.21 (t, 4H, J=8.1 Hz), 8.05 (m, 4H), 7.86 (t, 2H, J=5.9 Hz), 7.57 (m, 4H), 7.42 (m, 2H), 6.97 (d, 2H, J=8.4 Hz), 6.72 (d, 2H, J=8.4 Hz), 2.88 (t, 2H, J=7.2 Hz), 2.57 (s, 3H), 2.53 (t, 2H, J=7.2 Hz), 1.80-1.66 (m, 2H), 1.68-1.56 (m, 2H).

Acknowledgements

Tack till (Thanks to)…..

…..all the nice people that have been working at the department during these years, post docs, Ph.D. students, diploma workers etc and made it such an excellent working place.

.....special thanks to the JEB-group for letting me be a “half-member” for a long time, for ”pool-lunch”, Friday-beer and pizza etc. Och tack JEB för att du lät mig vara en riktig del av din grupp sista året.

.....min handledare Björn för all hjälp och stöd. Thanks to all the BÅ-group-members for support and help, special thanks to the post-docs who have been handling my help-need very well.

.....Berit, som styrde upp allt det här på ett helt suveränt sätt.

.....mina samarbetspartners och informella ”handledare” som tålmodigt delat med sig av sin entusiasm, tid och kunskap inom sina respektive ämne: Dick, Margareta, Micke, Cecilia och Leif.

.....Pino och Hasse för mycket betydelsefull diskussion, inspiration och uppmuntran.

.....de nya labkompisarna på lab 1.

.....all annan personal på insitutionen som har hjälpt mig och skapat lite ording i kaoset: Britt, data-Magnus, data-Ola, PU och Bertil m.fl. Stort tack till Kristina för all NMR-hjälp. Och tack Hillevi i bilioteket.

.....mina övriga samarbetspartners: De i konsortiet för artificiell fotosyntes: Tania och Reiner. Stort tack till Martin som ställde upp under avhandlingsskrivandet när det behövdes som bäst. Johan och Gabor på KTH.

.....konsortiet för artificiell fotosyntes, för den tid som blev.

.....the following people for reading and improving this thesis: Lars, Sascha, Jocke, Martin, Dick, Berit, Micke, Margareta.

.....C.F Liljevalchs j:ors stipendiefond och AstraZenecas resestipendium till minne av Nils Löfgren.

.....vännerna utanför universitetet. KTH-gänget: ni är så bra!

.....mina föräldrar och syskon och min släkt. Tack för att ni trott på mig.

.....min lilla familj, som ger en högre och större mening med allt det här♥

References

1. Diner Bruce, A.; Rappaport, F., *Annu. Rev. Plant Biol.* **2002,** 53, 551-580.
2. Loll, B.; Kern, J.; Saenger, W.; Zouni, A.; Biesiadka, J., *Nature* **2005,** 438, 1040-1044.
3. Kok, B.; Forbush, B.; McGloin, M., *Photochem. Photobiol.* **1970,** 11, 457-475.
4. Joliot, P.; Barbieri, G.; Chabaud, R., *Photochem. Photobiol.* **1969,** 10, 309-329.
5. Siegbahn, P. E. M.; Lundberg, M., *Photochem. Photobiol. Sci.* **2005,** 4, 1035-1043.
6. Lundberg, M.; Blomberg, M.; Siegbahn, P. E. M., *Inorg. Chem.* **2004,** 43, 264-274.
7. Siegbahn, P. E. M.; Crabtree, R. H., *J. Am. Chem. Soc.* **1999,** 121, 117-127.
8. Kalyanasundaram, K., *Photochemistry of Polypyridine and Porhyrine Complexes*. Academic Press Limited: London 1992.
9. O'Regan, B.; Graetzel, M., *Nature* **1991,** 353, 737-740.
10. Hagfeldt, A.; Graetzel, M., *Chem. Rev.* **1995,** 95, 49-68.
11. Hammarstrom, L., *Curr. Opin. Chem. Biol.* **2003,** 7, 666-673.
12. Vrettos, J. S.; Brudvig, G. W., *Comprehens. Coord. Chem. II* **2004,** 8, 507-547.
13. Limburg, J.; Vrettos, J. S.; Liable-Sands, L. M.; Rheingold, A. L.; Crabtree, R. H.; Brudvig, G. W., *Science* **1999,** 283, 1524-1527.
14. Naruta, Y.; Sasayama, M.-a.; Sadaki, T., *Angew. Chem.* **1994,** 106, 1964-1965.
15. Liu, X.; Ibrahim, S. K.; Tard, C.; Pickett, C. J., *Coord. Chem. Rev.* **2005,** 249, 1641-1652.
16. Sun, L.; Aakermark, B.; Ott, S., *Coord. Chem. Rev.* **2005,** 249, 1653-1663.
17. Ott, S.; Kritikos, M.; Akermark, B.; Sun, L.; Lomoth, R., *Angew. Chem., Int. Ed. Engl.* **2004,** 43, 1006-1009.
18. Zhao, X.; Georgakaki, I. P.; Miller, M. L.; Yarbrough, J. C.; Darensbourg, M. Y., *J. Am. Chem. Soc.* **2001,** 123, 9710-9711.
19. Hammarstrom, L.; Sun, L.; Akermark, B.; Styring, S., *Biochim. Biophys. Acta, Bioenergetics* **1998,** 1365, 193-199.
20. Lachaud, F.; Quaranta, A.; Pellegrin, Y.; Dorlet, P.; Charlot, M.-F.; Un, S.; Leibl, W.; Aukauloo, A., *Angew. Chem., Int. Ed. Engl.* **2005,** 44, 1536-1540.
21. Sjoedin, M.; Styring, S.; Kermark, B.; Sun, L.; Hammarstroem, L., *J. Am. Chem. Soc.* **2000,** 122, 3932-3936.
22. Burdinski, D.; Wieghardt, K.; Steenken, S., *J. Am. Chem. Soc.* **1999,** 121, 10781-10787.
23. Sun, L.; Burkitt, M.; Tamm, M.; Raymond, M. K.; Abrahamsson, M.; Le-Gourrierec, D.; Frapart, Y.; Magnuson, A.; Kenez, P. H.; Brandt, P.; Tran, A.; Hammarstroem, L.; Styring, S.; Aakermark, B., *J. Am. Chem. Soc.* **1999,** 121, 6834-6842.

24. Stryer, L., *Biochemistry*. 4 ed.; W. H. Freeman and Company: New York, 1995.
25. Desiraju, G.; Steiner, T., *The Weak Hydrogen Bond: Applications to Structural Chemistry and Biology*. 1999; p 528 pp.
26. Frey, P. A., *Magn. Reson. Chem.* **2001,** 39, S190-S198.
27. Sobczyk, L.; Grabowski, S. J.; Krygowski, T. M., *Chem. Rev.* **2005,** 105, 3513-3560.
28. Gilli, P.; Bertolasi, V.; Ferretti, V.; Gilli, G., *J. Am. Chem. Soc.* **1994,** 116, 909-915.
29. Gilli, P.; Bertolasi, V.; Pretto, L.; Antonov, L.; Gilli, G., *J. Am. Chem. Soc.* **2005,** 127, 4943-4953.
30. Steiner, T., *Angew. Chem., Int. Ed.* **2002,** 41, 48-76.
31. Emsley, J., *Chem. Soc. Rev.* **1980,** 9, 91-124.
32. Smith, M. B.; March, J., *Advanced organic chemistry*. 5 ed.; Wiley Interscience: New York, 2001.
33. Bagno, A.; Gerard, S.; Kevelam, J.; Menna, E.; Scorrano, G., *Chem. Eur. J.* **2000,** 6, 2915-2924.
34. Ferguson-Miller, S.; Babcock, G. T., *Chem. Rev.* **1996,** 96, 2889-2907.
35. Whittaker, J. W., *Arch. Biochem. Biophys.* **2005,** 433, 227-239.
36. Kolberg, M.; Strand, K. R.; Graff, P.; Kristoffer Andersson, K., *Biochim. Biophys. Acta, Proteins and Proteomics* **2004,** 1699, 1-34.
37. Nan, C. G.; Ping, W. X.; Ping, D. J.; Qing, C. H., *Talanta* **1999,** 49, 319-330.
38. Wang, H. L.; O'Malley, R. M.; Fernandez, J. E., *Macromolecules* **1994,** 27, 893-901.
39. Becke, A. D., *J. Chem. Phys.* **1993,** 98, 1372-1377.
40. Jensen, F., *Introduction to Computational Chemistry*. 1 ed.; John Wiley & Sons: Chichester, 1999.
41. Becke, A. D., *Phys. Rev. A: At., Mol., Opt. Phys.* **1988,** 38, 3098-3100.
42. Lee, C.; Yang, W.; Parr, R. G., *Phys. Rev. B: Condens. Matter Mater. Phys.* **1988,** 37, 785-789.
43. Vosko, S. H.; Wilk, L.; Nusair, M., *Can. J. Phys.* **1980,** 58, 1200-1211.
44. Becke, A. D., *J. Chem. Phys.* **1993,** 98, 5648-5652.
45. Gill, P. M. W.; Johnson, B. G.; Pople, J. A.; Frisch, M. J., *Int. J. Quantum Chem. Quant. Chem. Symp.* **1992,** 26, 319-331.
46. Perdew, J. P.; Wang, Y., *Phys. Rev. B* **1992,** 45, 13244-13249.
47. Bisht, P. B.; Tripathi, H. B.; Pant, D. D., *J. Photochem. Photobiol., A* **1995,** 90, 103-108.
48. Curtiss, L. A.; Raghavachari, K.; Redfern, P. C.; Pople, J. A., *J. Chem. Phys.* **2000,** 112, 7374-7383.
49. Curtiss, L. A.; Raghavachari, K.; Redfern, P. C.; Pople, J. A., *J. Chem. Phys.* **1997,** 106, 1063-1079.
50. Lozynski, M.; Rusinska-Roszak, D.; Mack, H.-G., *J. Phys. Chem. A* **1998,** 102, 2899-2903.
51. Tuma, C.; Daniel Boese, A.; Handy, N. C., *Phys. Chem. Chem. Phys.* **1999,** 1, 3939-3947.

52. Ireta, J.; Neugebauer, J.; Scheffler, M., *J. Phys. Chem. A* **2004,** 108, 5692-5698.
53. Rappe, A. K.; Bernstein, E. R., *J. Phys. Chem. A* **2000,** 104, 6117-6128.
54. Qin, Y.; Wheeler, R. A., *J. Chem. Phys.* **1995,** 102, 1689-1698.
55. Qi, X.-J.; Liu, L.; Fu, Y.; Guo, Q.-X., *Struct. Chem.* **2005,** 16, 347-353.
56. Jaguar 5.5, S., L.L.C., Portland, OR, **1991-2003**.
57. Altwicker, E. R., *Chem. Rev.* **1967,** 67, 475-531.
58. Bordwell, F. G.; Cheng, J., *J. Am. Chem. Soc.* **1991,** 113, 1736-1743.
59. Streitweiser, A.; Heathcock, C. H.; Kosower, E. M., *Introduction to Organic Chemistry* 4ed.; Macmillan Publishing company: 1992.
60. Land, E. J.; Porter, G.; Strachan, E., *Trans. Faraday Soc.* **1961,** 57, 1885-1893.
61. Dixon, W. T.; Murphy, D., *J. Chem. Soc., Faraday Trans. 2* **1976,** 72, 1221-1230.
62. Chang, C. J.; Chang, M. C. Y.; Damrauer, N. H.; Nocera, D. G., *Biochim. Biophys. Acta, Bioenergetics* **2004,** 1655, 13-28.
63. Mayer, J. M., *Annu. Rev. Phys. Chem.* **2004,** 55, 363-390.
64. Biczok, L.; Gupta, N.; Linschitz, H., *J. Am. Chem. Soc.* **1997,** 119, 12601-12609.
65. Fossey, J.; Lefort, D.; Sorba, J., *Free Radicals in Organic Chemistry*. 1 ed.; John Wiley & Sons, Masson: Chichester, 1995.
66. Richards, J. A.; Whitson, P. E.; Evans, D. H., *J. Electroanal. Chem. and Interfac. Electrochem.* **1975**, 311-327.
67. Hapiot, P.; Pinson, J.; Yousfi, N., *New J. Chem.* **1992,** 16, 877-881.
68. Maki, T.; Araki, Y.; Ishida, Y.; Onomura, O.; Matsumura, Y., *J. Am. Chem. Soc.* **2001,** 123, 3371-3372.
69. Qin, Y.; Wheeler, R. A., *J. Am. Chem. Soc.* **1995,** 117, 6083-6092.
70. Chaudhuri, P.; Wieghardt, K., *Prog. Inorg. Chem.* **2001,** 50, 151-216.
71. Westphal, K. L.; Tommos, C.; Cukier, R. I.; Babcock, G. T., *Curr. Opin. Plant. Biol.* **2000,** 3, 236-242.
72. Pujols-Ayala, I.; Barry, B. A., *Biochemistry* **2002,** 41, 11456-11465.
73. Blomberg, M. R. A.; Siegbahn, P. E. M.; Babcock, G. T., *J. Am. Chem. Soc.* **1998,** 120, 8812-8824.
74. Ahlbrink, R.; Haumann, M.; Cherepanov, D.; Boegershausen, O.; Mulkidjanian, A.; Junge, W., *Biochemistry* **1998,** 37, 1131-1142.
75. Tommos, C.; Babcock, G. T., *Biochim. Biophys. Acta, Bioenergetics* **2000,** 1458, 199-219.
76. Tang, X.-S.; Randall, D. W.; Force, D. A.; Diner, B. A.; Britt, R. D., *J. Am. Chem. Soc.* **1996,** 118, 7638-7639.
77. Mamedov, F.; Sayre, R. T.; Styring, S., *Biochemistry* **1998,** 37, 14245-14256.
78. Berthomieu, C.; Hienerwadel, R.; Boussac, A.; Breton, J.; Diner, B. A., *Biochemistry* **1998,** 37, 10547-10554.
79. Force, D. A.; Randall, D. W.; Britt, R. D.; Tang, X.-S.; Diner, B. A., *J. Am. Chem. Soc.* **1995,** 117, 12643-12644.

80. Hays, A. M.; Vassiliev, I. R.; Golbeck, J. H.; Debus, R. J., *Biochemistry* **1998,** 37, 11352-11365.
81. Hays, A.-M. A.; Vassiliev, I. R.; Golbeck, J. H.; Debus, R. J., *Biochemistry* **1999,** 38, 11851-11865.
82. Roffey, R. A.; Kramer, D. M.; Govindjee; Sayre, R. T., *Biochim. Biophys. Acta* **1994,** 1185, 257-270.
83. Roffey, R. A.; van Wijk, K. J.; Sayre, R. T.; Styring, S., *J. Biol. Chem.* **1994,** 269, 5115-5121.
84. Zouni, A.; Witt, H.-T.; Kern, J.; Fromme, P.; Krauss, N.; Saenger, W.; Orth, P., *Nature* **2001,** 409, 739-743.
85. Barber, J.; Ferreira, K.; Maghlaoui, K.; Iwata, S., *Phys. Chem. Chem. Phys.* **2004,** 6, 4737-4742.
86. Kamiya, N.; Shen, J.-R., *Proc. Natl. Acad. Sci. U. S. A.* **2003,** 100, 98-103.
87. Pesavento, R. P.; Van Der Donk, W. A., *Adv. Protein Chem.* **2001,** 58, 317-385.
88. Rutherford, A. W.; Boussac, A.; Faller, P., *Biochim. Biophys. Acta, Bioenergetics* **2004,** 1655, 222-230.
89. Juris, A.; Balzani, V.; Barigelletti, F.; Campagna, S.; Belser, P.; Von Zelewsky, A., *Coord. Chem. Rev.* **1988,** 84, 85-277.
90. O'Malley, P. J., *J. Am. Chem. Soc.* **1998,** 120, 11732-11737.
91. Wang, Y.-N.; Eriksson, L. A., *Int. J. Quantum Chem.* **2001,** 83, 220-229.
92. Fang, Y.; Liu, L.; Feng, Y.; Li, X.-S.; Guo, Q.-X., *J. Phys. Chem. A* **2002,** 106, 4669-4678.
93. Unpublished results
94. Catalan, J.; Fabero, F.; Soledad Guijarro, M.; Claramunt, R. M.; Santa Maria, M. D.; Foces-Foces, M. d. l. C.; Hernandez Cano, F.; Elguero, J.; Sastre, R., *J. Am. Chem. Soc.* **1991,** 113, 4046.
95. Fores, M.; Duran, M.; Sola, M.; Adamowicz, L., *J. Phys. Chem. A* **1999,** 103, 4413-4420.
96. Foces-Foces, C.; Llamas-Saiz, A. L.; Claramunt, R. M.; Cabildo, P.; Elguero, J., *J. Mol. Struct.* **1998,** 440, 193-202.
97. Costentin, C.; Robert, M.; Saveant, J.-M., *J. Am. Chem. Soc.* **2006,** 128, 4552-4553.
98. Zouni, A.; Jordan, R.; Schlodder, E.; Fromme, P.; Witt, H. T., *Biochim. Biophys. Acta, Bioenergetics* **2000,** 1457, 103-105.
99. Wakselman, M.; Robert, J. C.; Decodts, G.; Vilkas, M., *Bull. Soc. Chim. Fr.* **1973**, 1179-1183.
100. Gridnev, A. A.; Mihaltseva, I. M., *Synth. Commun.* **1994,** 24, 1547-1555.
101. Schuster, I. I.; Roberts, J. D., *J. Org. Chem.* **1979,** 44, 3864-3867.
102. Bachovchin, W. W., *Magn. Reson. Chem.* **2001,** 39, S199-S213.
103. Johnson, L. F.; Jankowski, W. C., *Carbon-13 NMR spectra*. John-Wiley & Sons, : New York, 1972.
104. Spiess, H. W., *Adv. Polym. Sci.* **1985,** 66, 23-58.
105. Thomas, F.; Jarjayes, O.; Jamet, H.; Hamman, S.; Saint, A.; Duboc, C.; Pierre, J.-L., *Angew. Chem., Int. Ed.* **2004,** 43, 594-597.
106. Rhile, I. J.; Mayer, J. M., *J. Am. Chem. Soc.* **2004,** 126, 12718-12719.

107. Dubowchik, G. M.; Padilla, L.; Edinger, K.; Firestone, R. A., *J. Org. Chem.* **1996,** 61, 4676-4684.
108. Negishi, E.; Zeng, X.; Tan, Z.; Qian, M.; Hu, Q.; Huang, Z., *Metal-Catalyzed Cross-Coupling Reactions*. 2 ed.; Wiley-VCH Weinheim, 2004; Vol. 2, p 815-889.
109. Lucarini, M.; Mugnaini, V.; Pedulli, G. F.; Guerra, M., *J. Am. Chem. Soc.* **2003,** 125, 8318-8329.
110. Serjeant, E. P.; Dempsey, B., *Ionization Constants of Organic Acids in Aqueous Solution* Pergamon Press: Oxford, 1970.